www.sciencemag.org/cgi/content/full/334/6063/1716/DC1

Supporting Online Material for

Model-Driven Engineering of RNA Devices to Quantitatively Program Gene Expression

James M. Carothers, Jonathan A. Goler, Darmawi Juminaga, Jay D. Keasling*

*To whom correspondence should be addressed. E-mail: keasling@berkeley.edu

Published 23 December 2011, *Science* **334**, 1716 (2011)
DOI: 10.1126/science.1212209

This PDF file includes:

Supporting Online Material for

Model-driven engineering of RNA devices to quantitatively-program gene expression

James M. Carothers, Jonathan A. Goler, Darmawi Juminaga and Jay D. Keasling*

*correspondence to: keasling@berkeley.edu

This PDF file includes:

Materials and Methods

Mechanistic modeling

Expression device function was modeled with a set of 25 chemical reactions (Fig. S2) implemented as differential equations coded and solved deterministically with the Dizzy ODE-RK5-adaptive solver (*31*) using custom software for set-up and analysis. Solving the system of equations gives the number of protein molecules (N_P) at time *t,* where for proteins with long half-lives N_P is directly related to the rate of protein production, *r*, integrated across the experiment. Static rRED expression is measured relative to a reference expression device *(14)* without a ribozyme, $\gamma_{rel} = r_{reg} / r_{ref}$. For aREDs, maximal dynamic ligand-dependent expression is taken as $\gamma_{rel} = r_{[L] >> sat} / r_{[L] << sat}$, [*L*] = ligand concentration (also see Fig. S2) (*9*). Parameter values in Tables S3, S4 and S6 were used to model predicted γ_{rel} for assembled expression devices. The variation in predicted γ_{rel} was estimated by bootstrapping from 1,000 replicates with parameter values taken randomly from Gaussian distributions (truncated at 0), with the values in Tables S3, S4, and S6 as approximations of μ and σ.

Monte Carlo filtering and global sensitivity analysis

Monte Carlo filtering (*15*) was employed to map the relationships between the space of design variable inputs, $x = [x_1, x_2, ... , x_n]$, where the elements correspond to the design variables, and the space of expression device outputs, $y(x) = [y_1(x), y_2(x), ... , y_n(x)]$, where the elements correspond to γ_{rel}. 4×10^4 sets of differential equations were solved with Monte Carlo distributions of parameter values generated over the intervals shown in Table S1. For rREDs, equations with matched sets of parameter values and $k_{obs-} = 0$ were solved to determine r_{ref} and compute γ_{rel}. For aREDs, equations with matched sets of parameter values and $k_{obs+} = 0$ were solved to determine $r_{[L] << sat}$ and compute γ_{rel}. To perform global sensitivity analysis, partial rank correlation coefficients (PCCs) were computed with R (R Foundation

for Statistical Computing, Vienna, Austria), using those data to measure the contribution of individual design variables x_i on device function *y,* without the effects of the other elements of x. Application of the rank transformation was indicated by the non-linear, generally monotonic relationships observed between the x_i and *y* (*32*). PCCs were computed with R and 95% confidence intervals were estimated from bootstrap replicates (10 replicates with sample size = 4×10^4). To identify the space of design variable inputs consistent with targeted levels of expression, parameter inputs were filtered by device outputs (γ_{rel}) with bin sizes = 0.25 (minimum number of samples per bin > 50) and the resulting curves were fit with third order polynomial splines using R.

Ribozyme and aptazyme *in vitro* cleavage rates

The ribozyme and aptazyme sequences shown in Fig. S4 were transcribed from PCR-amplified chemically-synthesized DNA templates with 50 U/µl of T7 RNA polymerase in 40 mM Tris-HCl (pH 7.8) with 20 mM each NTP, 25 mM Mg^{2+}, 2.5 mM spermidine, 10 mM DTT, 0.01% Triton X-100, 10 U/µl thermostable inorganic pyrophosphatase (TIPP, New England Biolabs, Inc.) and 200 U/µl RNAsin (Promega, Inc.) and 0.1 µCi of ^{32}P-ATP. To minimize ribozyme self-cleavage during transcription, 2 µM 'blocking oligos' complementary to the 5' end of ribozyme were added to the transcription reactions (*33*). Blocking oligo sequences were as follows: ASBV-1, 2, 3: 5'-GTC TCT TCA GGG ATA G-3'; vLTSV-1, 2: 5'-GGG CCA TCT TCA GTG AGC GGG-3'; sTRSV-1, 2, 3, 4: 5'-GGA CTC ATC AGA CCG G-3'; PLMVd: 5'-CTC AGA GAC TCG TCA GTG TGC-3; HH2: 5'-TCG GCC TCA TCA GGT CAT CGC-3'. RNAs were purified on an 8% PAGE gel, electroeluted, and ethanol precipitated with KCl.

Ribozymes were heated to 65°C for 1 min and subsequently incubated at 30°C in 1 mM $MgCl_2$, 10 mM Tris-HCl, pH 7.5 and 0.05 mM EDTA. Theophylline aptazymes were heated to 65°C for 1 min

and subsequently incubated at 30°C in 1 mM $MgCl_2$, 10 mM Tris-HCl, pH 7.5 and 0.05 mM EDTA with or without 3 mM theophylline. *p*-AF aptazymes were incubated at 30°C in 1 mM $MgCl_2$, 130 mM k-glutamate, pH 7.5, 15 mM NaCl and 10 mM DTT with or without 5 mM *p*-amino-DL-phenylalanine (*p*-AF, Sigma, Inc.). Over at least 4 time intervals (ranging from 1 min to as long as 150 min), the cleavage reactions were quenched by the addition of an equal volume of stop solution (95% formamide and 5% 0.5 M EDTA, v/v %); reaction products were resolved with PAGE and visualized by phosphoimager scanning. Self-cleavage rate constants were determined by fitting an exponential unimolecular decay curve to the fraction of RNA cleaved as a function of time (*18*) using R.

RNA folding simulations and transcript design

Kinetic, co-transcriptional, RNA secondary structure folding simulations of helix formation and dissociation were conducted by implementing the kinefold_long_static binary (*22*) with custom software for set-up and analysis. Simulations were performed with helix minimum free energy = 6.346 kcal/mol and no pseudoknots or entanglements.

To design transcripts, libraries of L_{spc} and R_{spc} hexamers were searched to identify spacer sequences that enable RBS and ribozyme (or aptazyme) folding, as measured by the mean normalized distance score for a set of devices, where $d = 1 - \sqrt{((1 - f_{rbz})^2 + (1 - f_{rbs})^2)/2}$. f_{rbz} = predicted ribozyme folding frequency, taken as the fraction of transcripts given spacer sequences $L_{spc} = x_i$ and $R_{spc} = y_j$ with ribozymes folded into target secondary structures. f_{rbs} = predicted ribozyme and RBS folding frequency, taken as the fraction of transcripts given spacer sequences x_i and y_j with ribozyme and RBS sequences folded into target secondary structure(s). Target ribozyme secondary structures are presented in Fig. S4 (see Table S4 for discussion of target aptazyme secondary structures). Target RBS secondary structure(s) were defined as the ensemble of secondary structure outputs obtained through folding

simulations of reference device transcripts with spacer sequences x_i and y_j. 200 co-transcriptional kinetic folding simulations were initiated with random seeds for each expression device and spacer sequence permutation (100 simulations each for a low and high polymerase elongation rate, k_{pol}) and the RBS (f_{rbs}) and ribozyme (f_{rbz}) folding frequencies determined from the set of secondary structure outputs. For T7 RNA polymerase low k_{pol} = 97 nt/s and high k_{pol} = 200 nt/s. For *E. coli* RNA polymerase low k_{pol} = 25 nt/s and high k_{pol} = 55 nt/s (see Table S1). The simulation time was set for each expression device transcript as t_1 = len(U_{ppp}) / k_{pol}, where len(U_{ppp}) = (length from 5' end to RBS center) + (k_{pol} · 1 s), where 1 s approximates the shortest time for a ribosome to interact productively with an RBS (Table S1, references therein).

To design transcripts for rREDs expressing RFP, R_{spc} was fixed as 5'-AGATCT-3' (BglII restriction enzyme recognition sequence). L_{spc} was varied across 21 hexamers corresponding to the common restriction enzyme recognition sites absent from the prRED0-T7-ref expression device plasmid. As described above, 100 folding simulations were performed for each L_{spc} permutation for the reference device and rRED transcripts with the low and high T7 RNA polymerase k_{pol}. To design transcripts for rREDs expressing the *papABC* operon, L_{spc} was fixed as 5'-GAATTC-3' (EcoRI). R_{spc} was varied across 15 hexamers corresponding to the common restriction enzyme recognition sites absent from the prRED14-lac-ref expression device plasmid. 100 folding simulations were performed with low and high *E. coli* k_{pol} for each permutation.

To predict ribozyme or aptazyme folding rates (k_{fold}), 4 individual runs of 100 simulations for each expression device were initiated with random seeds and T7 RNA polymerase k_{pol} = 97 nt/s and *E. coli* polymerase k_{pol} = 25 nt/s. t_1, as above, was the first simulation time interval; t_2 = 17.5 s, t_3 = 35 s, and t_4 = 70 s (half-life of the rRED-pPro-ref mRNA). k_{fold} was determined from an exponential fit of the fraction of transcripts with ribozymes or aptazymes folded into target secondary structures as a

function of time using R (mean relative variance = 0.035).

RNA half-life measurements

After overnight growth shaking at 200 rpm at 37°C, cultures were diluted 1:100 into fresh media. Transcription was induced after 1.5-2 hours of growth in culture tubes shaking at 200 rpm at 30°C. At OD600=0.4, transcription inhibition was initiated by the addition of 250 μg/ml of rifampicin in DMSO (*34*). Cells were harvested at 0, 2.5, 7.5 and 17.5 minutes by adding an equal volume of stop solution (10% phenol and 90% ethanol, v/v %), vortexing briefly and freezing at -80°C. Cells were thawed on ice, pelleted by centrifugation at 14K × g for 1 min at 4°C. After removing the supernatant, equal volumes of 0.1 mm diameter glass beads and RTL buffer (Qiagen, Inc.) were added to the cell pellet. After shaking at 30 orbits/sec for 4 min, the beads were pelleted by centrifugation. RNA was purified from the supernatant using Qiagen RNeasy column protocols. RNA was subsequently treated with RQ1 DNase (Promega, Inc.) and re-purified using a second Qiagen RNEasy column. Transcript abundance was measured with quantitative RT-PCR using Applied Biosystems, Inc. Power SYBR enzyme mixes and comparison to endogenous 16S rRNA levels (which were not observed to change). RT-qPCR primers were designed with Applied Biosystems, Inc. Primer Express software. Primers for amplifying 16S RNA were: 5'-GTG GCA TTC TGA TCC ACG ATT AC-3' and 5'-CCG GAT TGG AGT CTG CAA CT -3'. Primers for amplifying RFP RNA were 5'-CAT CCT GTC CCC GCA GTT-3' and 5'-GTC AGC CGG GTG TTT AAC GT-3'. Primers for amplifying *papA* RNA were 5'-ATT TCA GAA TTC AAA TGT ACA GAT TCA CAC ACA GGA AAC AGC T-3' and 5'-TCG CCG ATG TAC TGG AAC AG-3'. RNA degradation rate constants were determined by fitting an exponential unimolecular decay curve to the fraction of RNA degraded as a function of time using R.

Plasmid construction

All DNA manipulations were carried out in *E. coli* DH10B (Life Technologies, Inc.) with well-established protocols. Briefly, sequences for the promoters, L_{spc} and R_{spc}, ribozymes and aptazymes were PCR-amplified from overlapping, chemically-synthesized oligonucleotides with primers flanked by restriction enzyme sites enabling digestion and ligation into plasmid vectors. The ribosome binding site (B0034) and open reading frame for rREDs and aREDs expressing RFP were PCR-amplified from part BBa_J61002, identified as an 'RFP reporter' in the Registry of Standard Biological Parts (www.partregistry.org). The ribosome binding sites and open reading frames for the engineered *papABC* operon were PCR-amplified from the pLASC-lacpw plasmid (*27*), obtained from J.C. Anderson (UC Berkeley). Construct assemblies were confirmed by sequencing. Expression device plasmids (Fig. S6) will be available from www.addgene.org upon publication.

rRED and aRED programmed RFP expression

Plasmids bearing rREDs and aREDs expressing the DsRed (RFP) open reading frame (Fig. S6) were transformed into *E. coli* BL21 (DE3) (Novagen, Inc.). Liquid culture conditions were Luria-Burtani (LB) with either 100 μg/ml of carbenicillin or 50 μg/ml of kanamycin. After overnight growth at 37°C, cultures were diluted 1:100 into fresh media and grown with shaking at 200 rpm in culture tubes at 30°C. Expression from the $P_{prp}B$ promoter was induced with 50 mM sodium propionate, pH 8.0 (*11*). Expression from the T7 promoter was induced with 1 mM IPTG. For aREDs, ligand was added to the culture medium upon transcription induction. RFP fluorescence (excitation = 557 nm, emission=579 nm) was measured after 18-24 hours of incubation at 30°C as a function of optical density (OD). At least three biological replicates were performed for each expression device and for each concentration of ligand.

p-AF aptazyme selection

A library of 10^8 PCR-amplified, chemically-synthesized DNA templates was *in vitro* transcribed in 15 minute reactions with T7 RNA polymerase and gel purified as above. The transcribed portion of the library sequences consisted of the *S. mansoni* ribozyme and the *p*-AF-R1-1 aptamer (*19*) with 14 completely-randomized nucleotides (N) in the stem 'bridge' regions (*18*), corresponding to the positions highlighted in blue, red and orange in the *p*-AF aptazyme sequences and structures shown in Fig. S4B. The oligonucleotides for pool generation were: LSW-11F, 5'-GCT AAT ACG ACT CAC TAT AGG CG AAA GCC GGC GCG TCC TGG ATT CCA CNN NNN CAT GTC CCT ACC ATA CGG GAT TGC CCA GC TTC GGC TGC CAT GCC GGC-3'; LSW-11Rc, 5'-AGC GCG TTT CGT CCT ATT TGG GAC TCA TCA GCN NNNT GTA CCN NNN NCG TAG GCC GGT TAC CGT TTG GCC GGC ATG GCA GCC G-3'. Primers for RT-PCR amplification were LSW-11Fp, 5'-GCT AAT ACG ACT CAC TAT AGG CGA AAG CCG GCG CGT CCT GGA TTC CAC-3' and LSW-11Rp, 5'-AGC GCG TTT CGT CCT ATT TGG G-3'.

To enrich for aptazyme sequences that catalyze *p*-AF-dependent self-cleavage reactions, full-length RNA was resuspended in selection buffer (SB, 130 mM potassium glutamate, pH 7.5, 15 mM NaCl, 10 mM DTT and 1 mM $MgCl_2$) and incubated with 2mM *p*-AF for 1 hour at 20°C. The cleavage reactions were quenched by the addition of an equal volume of stop solution (95% formamide and 5% 0.5 M EDTA, v/v %). Cleaved RNA was PAGE purified on an 8% gel, electroeluted and precipitated with ethanol and KCl. Double-stranded DNA (dsDNA) templates were generated by RT-PCR and subsequently *in vitr*o transcribed. To select for aptazyme sequences that cleaved slowly in the absence of ligand (slow k_{obs-}), full-length RNAs were PAGE purified and incubated in SB without *p*-AF. After 1 hour of incubation at 20°C, the uncleaved RNA was PAGE purified on an 8% gel. dsDNA was regenerated for the next round of *in vitro* selection by RT-PCR.

After 5 cycles of *in vitro* selection, the enriched pool of molecules was screened for ligand-

dependent aptazyme cleavage using an *in vivo* screen. The enriched library of sequences was amplified with cloning adapters and subcloned into prRED0-T7-ref (Fig. S6B). The cloning adapter primers were: Adapter4A.F, 5'-GAT ATC ATC TCT AGA GGC GAA AGC CGG CGC GTC CTG GAT TCC AC-3'; Adapter4AR, 5'-GAC CTT AGA TCT AGC GCG TTT CGT CCT ATT TGG G-3'. Plasmids were transformed into *E. coli* TOP 10 cells (Invitrogen, Inc.), miniprepped using standard protocols (Qiagen, Inc.) and re-transformed into *E. coli* BL21 cells. Individual colonies were picked into LB media with 50 μg/mL kanamycin (LB-kan) and grown overnight at 37˚C with 200 rpm of shaking. Each overnight culture was diluted 1:100 into two tubes of fresh LB+kan, one of which contained 5 mM *p*-AF. Expression from the T7 promoter was induced by the addition of 1 mM IPTG. Plasmids from cultures that gave increased *p*-AF-dependent RFP expression compared to the negative control after 24 hours of incubation at 30˚C with 200 rpm of shaking were isolated and sequenced to yield *p*-AF aptazymes (Fig. S4B).

rRED programmed *p*-AF production

Ampicillin-resistant plasmids bearing rREDs expressing the *papABC* operon (*10*)(Fig. S6) were transformed into an *E. coli* MG1655-derived strain engineered to overproduce chorismate using a modular two-plasmid system. One plasmid, pBb-Shik5 (chloramphenicol resistant) expresses genes for producing shikimate from glucose in two operons: $P_{Lac-UV5}$-*aroE-aroD-aroB* and $P_{Ltet-01}$-*aroG*-ppsA-tktA*, where *aroG** is a feedback insensitive version of *aroG*. The second plasmid, pBb-Cha (kanamycin resistant) expresses genes for producing chorismate from shikimate in a single operon: $P_{Lac-UV5}$-*aroC-aroA-aroL*. Liquid culture conditions were MOPS M9 minimal medium with 0.5% glucose (*36*) and 100 μg/ml of carbenicillin, 30 μg/ml of chloramphenicol and 50 μg/ml of kanamycin. After overnight growth at 30°C in tubes shaking at 200 rpm, cultures were diluted 1:100 into fresh medium

supplemented with 50μM IPTG to induce expression from $P_{Lac\text{-}UV5}$ ($P_{Ltet\text{-}01}$ is constitutively expressed).

1 ml of culture was extracted 30 hours post-induction with 1 ml of ice cold methanol. The samples were briefly vortexed and centrifuged at 14K × g for 30 minutes at 4°C. The amount of *p*-AF in the supernatant was monitored by HPLC using an Agilent, Inc. microbore system equipped with a photodiode array detector set at 280nm. *p*-AF was separated on a reverse-phase column with water (solvent A) and methanol as the mobile phase (solvent B) at a flow rate of 0.15 ml/min. The gradient was as follows: 1st step from 0 to 8 min, 95% A + 5% B; 2nd step from 8 to 13 min, B ratio was increased to 40%; 3rd step, B was held constant for 3 min; finally, the gradient was returned to 5% B in 5 min and held constant for an additional 10 min to equilibrate. The concentration of *p*-AF was determined by comparison with a standard curve generated with commercially-prepared *p*-AF (Sigma, Inc.)

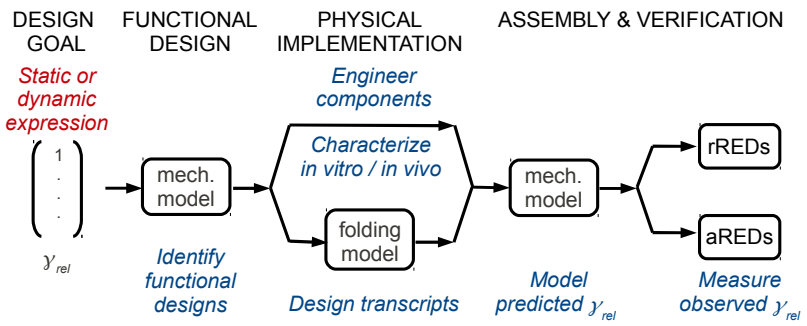

Fig. S1. Design-driven engineering process. Coarse-grained mechanistic modeling identifies design parameters to produce targeted device outputs. Components meeting the design specifications are then engineered and individually characterized. Transcripts are designed with kinetic RNA folding simulations, enabling the assembly of component parts into physical devices. Finally, device functions predicted from the parameter inputs (predicted y_{rel}) are verified by comparison to measured outputs (observed y_{rel}).

A

Txn/Trans				Rbz processing				Degradation			
	$\rightarrow I$	$, k_1$	(R1)	U_{ppp}	$\rightarrow U_{ppp,\ fold}$	$, k_6$	(R13)	U_{ppp}	$\rightarrow \emptyset$	$, k_9$	(R19)
I	$\rightarrow U_{ppp}$	$, k_2$	(R2)	$U_{ppp,\ fold}$	$\rightarrow U_{OH}$	$, k_7$	(R14)	$U_{ppp,\ fold}$	$\rightarrow \emptyset$	$, k_9$	(R20)
U_{ppp}	$\rightarrow R_{ppp}$	$, k_3$	(R3)	$U_{ppp,\ fold}$	$\rightarrow U_{OH}$	$, k_8$	(R15)	R_{ppp}	$\rightarrow \emptyset$	$, k_9$	(R21)
U_{OH}	$\rightarrow R_{OH}$	$, k_3$	(R4)	R_{ppp}	$\rightarrow R_{ppp,\ fold}$	$, k_6$	(R16)	$R_{ppp,\ fold}$	$\rightarrow \emptyset$	$, k_9$	(R22)
$U_{ppp,\ fold}$	$\rightarrow R_{ppp,\ fold}$	$, k_3$	(R5)	$R_{ppp,\ fold}$	$\rightarrow R_{OH}$	$, k_7$	(R17)	U_{OH}	$\rightarrow \emptyset$	$, k_{10}$	(R23)
U_{ppp}	$\rightarrow U_{ppp} + T$	$, k_4$	(R6)	$R_{ppp,\ fold}$	$\rightarrow R_{OH}$	$, k_8$	(R18)	R_{OH}	$\rightarrow \emptyset$	$, k_{10}$	(R24)
$U_{ppp,\ fold}$	$\rightarrow U_{ppp,\ fold} + T$	$, k_4$	(R7)					P	$\rightarrow \emptyset$	$, k_{11}$	(R25)
U_{OH}	$\rightarrow U_{OH} + T$	$, k_4$	(R8)								
R_{ppp}	$\rightarrow R_{ppp} + T$	$, k_4$	(R9)								
$R_{ppp,\ fold}$	$\rightarrow R_{ppp,\ fold} + T$	$, k_4$	(R10)								
R_{OH}	$\rightarrow R_{OH} + T$	$, k_4$	(R11)								
T	$\rightarrow P$	$, k_5$	(R12)								

B

$$\frac{d}{dt}\begin{pmatrix} I \\ U_{ppp} \\ U_{OH} \\ T \\ R_{ppp} \\ R_{OH} \\ U_{ppp,\ fold} \\ R_{ppp,\ fold} \\ P \end{pmatrix} = \begin{pmatrix} k_1 \\ 0 \\ 0 \\ 0 \\ 0 \\ 0 \\ 0 \\ 0 \\ 0 \end{pmatrix} + \begin{pmatrix} 0 & -k_2 & 0 & 0 & 0 & 0 & 0 & 0 & 0 \\ k_2 & -(k_3+k_6+k_9) & 0 & 0 & 0 & 0 & 0 & 0 & 0 \\ 0 & k_7+k_8 & -(k_3+k_{10}) & 0 & 0 & 0 & 0 & 0 & 0 \\ 0 & k_4 & k_4 & 0 & k_4 & k_4 & k_4 & k_4 & -k_5 \\ 0 & k_3 & 0 & 0 & -(k_6+k_9) & 0 & 0 & 0 & 0 \\ 0 & 0 & k_3 & 0 & k_7+k_8 & k_{10} & 0 & 0 & 0 \\ 0 & k_6 & 0 & 0 & 0 & 0 & -(k_3+k_7+k_8+k_9) & 0 & 0 \\ 0 & 0 & 0 & 0 & k_6 & 0 & k_3 & -(k_7+k_8+k_9) & 0 \\ 0 & 0 & 0 & k_5 & 0 & 0 & 0 & 0 & -k_{11} \end{pmatrix} \begin{pmatrix} I \\ U_{ppp} \\ U_{OH} \\ T \\ R_{ppp} \\ R_{OH} \\ U_{ppp,\ fold} \\ R_{ppp,\ fold} \\ P \end{pmatrix}$$

Species

I	Transcription initiation complex
U_{ppp}	5'PPP-untranslated RNA (5'UTR)
$U_{ppp,\ fold}$	5'PPP-untranslated RNA, ribozyme 2° structure folded
U_{OH}	5'OH-untranslated RNA (5'UTR)
R_{ppp}	5'PPP-RNA transcript (5'UTR and ORF)
$R_{ppp,\ fold}$	5'PPP-RNA transcript, ribozyme 2° structure folded
R_{OH}	5'OH-RNA transcript (5'UTR and ORF)
T	Translation initiation complex
P	Protein

Fig. S2. Expression device model. The rRED and aRED kinetic framework was formulated as a set of 25 chemical reactions (**A**) and is shown as reaction rate equations in matrix form (**B**) with the molecular species and rate constants given as in Fig. 1. Brief explanation follows.

A zero-order rate (k_1) describes transcription initiation frequency, while the transcript elongation phase is divided into two parts. k_2 is the rate constant for transcription of RNA to the end of the 5' portion containing the ribozyme or aptazyme and the ribosome binding site (RBS) (U_{ppp})(Fig. 1). Rate constants for transcript elongation have parameters for RNA polymerase elongation rate and transcript length (Table S1, below). Once the nascent U_{ppp} species has been transcribed, ribosomes can bind to the RBS and initiate transcription (k_4); ribozyme (or aptazyme) folding into the target secondary structure necessary for catalysis occurs with rate k_6. Apparent rate constants for ribozyme (or aptazyme) self-cleavage in the absence ($k_7 = k_{obs-}$) or presence ($k_8 = k_{obs+}$) of ligand capture remaining folding and catalytic events ($k_8 = k_7$ for ribozymes without aptamers). Ribozyme or aptazyme self-cleavage produces U_{OH} from U_{ppp}. U_{ppp} and U_{OH} are elongated by RNA polymerase to form full-length transcripts, R_{ppp} and R_{OH}, respectively, with rate k_3. 5'PPP terminated RNAs (U_{ppp}, $U_{ppp,fold}$, R_{ppp}, and $R_{ppp,fold}$) are degraded with rate k_9, while 5'OH terminated RNAs (U_{ppp} and U_{OH}) are degraded with rate k_{10}. k_5 and k_{11} are rate constants for protein translation (related to parameters for polypeptide elongation rate and ORF length) and protein degradation, respectively.

Solving the set of equations deterministically gives the number of protein molecules (N_P) at time t, from which the rate of protein production can be derived and described simply as $r = \alpha R - \beta P$, where R = mRNA concentration, α = an effective rate for protein synthesis, P = protein concentration and β = an effective rate for protein degradation. rREDs are engineered to program regulated gene expression rates relative to a reference expression device without a ribozyme such that $\gamma_{rel} = r_{reg} / r_{ref}$ (*14*). aREDs are engineered to program ligand-dependent gene expression such that $\gamma_{rel} = r_{[L]>>sat} / r_{[L]<<sat}$, $[L]$ = ligand concentration (*9*).

For aRED device outputs generated with intermediate ligand concentrations, where $r_{[L]}$ is smaller than $r_{[L]>>sat}$ but larger than $r_{[L]<<sat}$, k_8 is taken as the apparent aptazyme cleavage rate (k_{app})

given an effective concentration (*EC*) of ligand:

$$k_{app} = \frac{1}{(1 + \frac{EC_{50}}{[L]})} (k_{obs+} - k_{obs-}) + k_{obs-}$$

such that,

at $[L] = EC_{50}$, k_{app} is half maximal (halfway between k_{obs-} and k_{obs+})

at $[L] << EC_{50}$, $k_{app} = k_{obs-}$

at $[L] >> EC_{50}$, $k_{app} = k_{obs+}$.

Table S1. Parameter descriptions and intervals for global sensitivity analysis.

Rate constant	Description	Relationship to design variables	Parameter intervals	References
k_1	Txn init.	$k_1 = 1/t$	t = 0.0001 to 1	(*37*)
k_2	Txn elong. (U_{ppp})	$k_2 = \ln(2) / (½ * (d / k_{pol}))$	d[a] = 98-350 nts, k_{pol} = 25-230 nt·s^{-1}	(*38-40*)
k_3	Txn elong. (R_{ppp}/R_{OH})	$k_3 = \ln(2) / (½ * (d / k_{pol}))$	d[a] = 500-5000 nts, k_{pol} = 25-230 nt·s^{-1}	(*38-40*)
k_4	Trans init.	$k_4 = \ln(2) / (½ * (t))$	t[b] = 2-2000 s	(*41,42*)
k_5	Translation	$k_5 = \ln(2) / (½ * (d / k_{trans}))$	d = 500-5000 nts, k_{trans}[c] = 21-63 nt·s^{-1}	(*38,39*)
k_6	Rbz folding	$k_6 = k_{fold}$	k_{fold} = 0.0001-3 s^{-1}	(*43*)
k_7	(-) ligand rbz catalysis	$k_7 = k_{obs-}$	k_{obs-} = 0.001-10 min^{-1}	(*18,44*)
k_8	(+) ligand rbz catalysis	$k_8 = k_{obs+}$	k_{obs+} = 0.001-10 min^{-1}	(*18,44*)
k_9	5'PPP-RNA deg.	$k_9 = \ln(2) / t_{1/2, ppp}$	$t_{1/2, ppp}$ = 15 s-24 hrs	(*45*)
k_{10}	5'OH-RNA deg.	$k_{10} = \ln(2) / t_{1/2, OH}$	$t_{1/2, OH}$ = 15 s-24 hrs; $k_{10} = 0.1745 \cdot k_9$	(*13,46*)
k_{11}	Protein deg.	$k_{11} = \ln(2) / t_{1/2}$	$t_{1/2}$ = 60 s-24 hrs	(*47*)

[a] d = length of RNA (in nucleotides, nt), k_{pol} = RNA polymerase elongation rate

[b] ribosome binding and clearance of the ribosome binding site

[c] k_{trans} = translation elongation rate

Table S2. Global sensitivity analysis partial rank correlation coefficients (PCCs).

Design variable	PCC rREDs			Bias	PCC aREDs			Bias
$k_{init,\ txn}$	-0.110	±	0.007	9.42E-004	0.157	±	0.006	1.41E-003
k_{pol}	0.093	±	0.005	-2.29E-003	-0.007	±	0.007	2.55E-003
ORF	-0.010	±	0.003	-1.20E-003	0.003	±	0.004	1.11E-003
$k_{init,\ trans}$	-0.076	±	0.005	1.01E-003	0.163	±	0.006	2.15E-004
k_{fold}	0.170	±	0.007	-1.23E-003	0.038	±	0.008	-1.46E-003
k_{obs-}	0.658	±	0.003	-1.78E-003	-0.843	±	0.001	-9.02E-004
k_{obs+}					0.289	±	0.003	-4.13E-004
$RNA_{t1/2}$	0.509	±	0.007	1.49E-003	-0.684	±	0.003	1.70E-003
$Protein_{t1/2}$	-0.071	±	0.008	-1.10E-003	0.154	±	0.007	4.31E-004

± s.e. is shown for the PCCs (*15, 22*) computed between each design variable and y_{rel}.

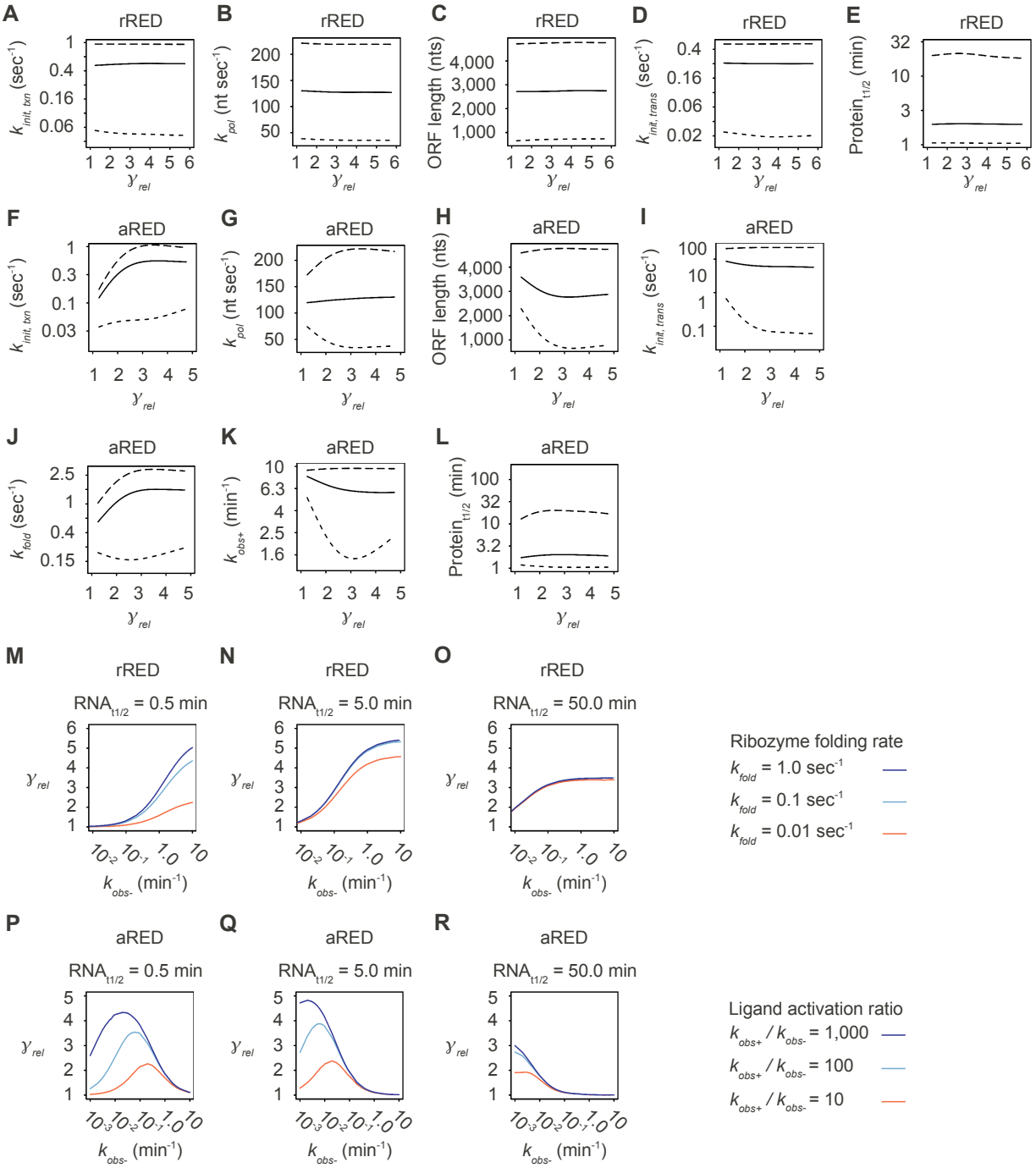

Fig. S3. Monte Carlo filtering and design variable space mapping. Sampling-based mappings of design variable spaces filtered by γ_{rel}. Median (**—**), 5th (**- -**) and 95th (**– –**) %-tile for design variables not shown in Fig. 1 are given: (**A-E**) design variables for rREDs. (**F-L**) design variables for aREDs. (**M-O**) rRED γ_{rel} for the expression of red fluorescent protein with T7 RNA polymerase (see Table S6 for parameter values) is plotted as a function of ribozyme cleavage rate (k_{obs-}) and ribozyme folding rate (k_{fold}), for short, medium and long half-lives (RNA$_{t1/2}$ = 0.5, 5.0 and 50 min, respectively). (**P-R**) aRED γ_{rel} for the expression of red fluorescent protein with T7 RNA polymerase is plotted as a function of no-ligand cleavage rate (k_{obs-}) and ligand-activation ratio (k_{obs+} / k_{obs-}) for RNAs with short, medium and long RNA$_{t1/2}$.

A Hammerhead ribozymes

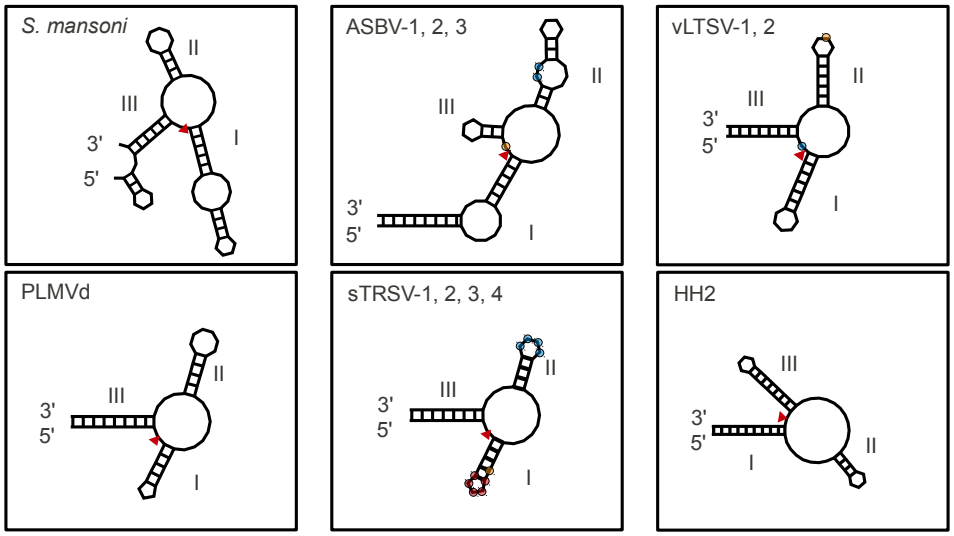

Hammerhead ribozymes

>*S. mansoni*
gggcgaaagccggcgcguccuggauuccacugcuucggcagguacauccagcugaugagucccaaauaggacgaaacgcgcu
.(((....))).((((((.((((((....((((....))))....))))))).......((((......)))).....)))))).
>ASBV-1
gggacgggccaucaucuaucccugaagagacgaaggcuucggccaagucgaaacggaaacgucggauagucgcccguccc
(((((((((......((((((.......(((...(((....)))..)))...(((....))).)))))))..)))))))))
>ASBV-2
gggacgggccaucaucuaucccugaagagacgaaggcuucggccAgucgaaacggaaacgucggauagucgcccguccc
(((((((((......((((((.......(((...(((....)))..)))...(((....))).)))))))..)))))))))
>ASBV-3
gggacgggccaucaucuaucccugaagagacgaaggcuucggccUCgucgaaacggaaacguGggauagucgcccguccc
(((((((((......((((((.......(((...(((....)))..)))...(((....))).)))))))..)))))))))
>vLTSV-1
ggguacgucugagcgugauacccgcucacugaagauggcccgguagggccgaaacguaccc
(((((((.(((((((.....)))))))).......((((((....))))))..)))))))
>vLTSV-2
ggguacguUgagcgugauacccgcucacugaagauggcccgAuagggccgaaacguaccc
(((((((.((((((.....))))))).......((((((....))))))..)))))))
>PLMVd
gggaagagucugugcuaagcacacugacgagucucugagaugagacgaaacucuuccc
(((((((((.((((((...))))))).......((((......))))))...)))))))))
>sTRSV-1
gggccugucaccgguaaccggucugaugaguccgugaggacgaaacaggccc
(((((((.((((((...))))))).......((((....))))))...)))))))
>sTRSV-2
gggccugucaccggAUGUGCUUUccggucugaugaguccCUGAAAUGggacgaaacaggccc
(((((((.((((((.......))))))).......((((......))))))...)))))))
>sTRSV-3
gggccugucaccggUAAccggucugaugaguccCUGAAAUGggacgaaacaggccc
(((((((.((((((...))))))).......((((((....))))))...)))))))
>sTRSV-4
gggcugucaccggAUGUGCUUUccggucugaugaGCCGGaggacgaaacagccc
(((((((.((((((.......))))))).......(((...)).)...)))))))
>HH2
gggcgaugaccugaugaggccgaaaggccgaaaggccgaaacguucucgcgagagaacgucgucgucgccc
((((((((((.......(((....))))..........(((((((((....)))))))).))))))))))

B Aptazymes

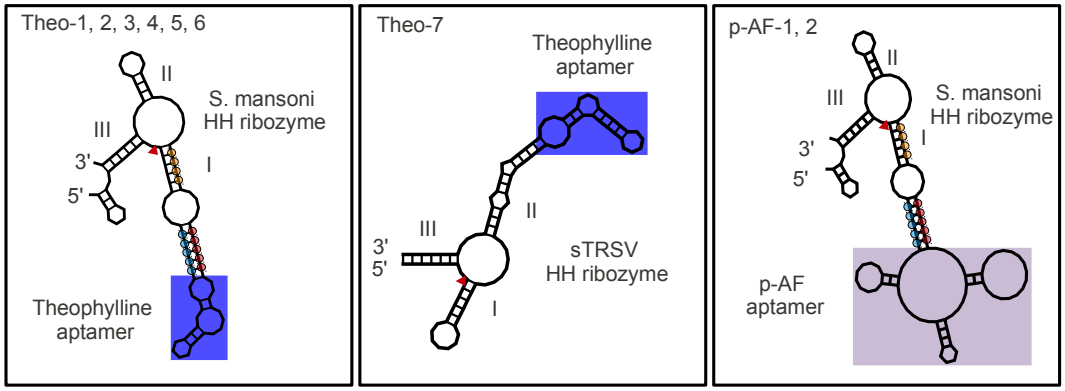

Theophylline aptazymes

>Theo-1
gggcgaaagccggcgcguccuggauuccacGAGAUAUACCAGCCGAAAGGCCCUUGGCAGCUCCCggaacaACCUgcugacgagucccaaauaggacgaaacg
cgcu
>Theo-2
gggcgaaagccggcgcguccuggauuccacCCGAGAUACCAGCCGAAAGGCCCUUGGCAGCUCCCggAacaACCUgcugaugagucccaaauaggacgaaacg
cgcu
>Theo-3
gggcgaaagccggcgcguccuggauuccacAUGUAUACCAGCCGAAAGGCCCUUGGCAGACUUUgguacaUGAAgcugaugagucccCaaauaggacgaaacg
cgcu
>Theo-4
gggcgaaagccggcgcguccuggauuccacAAUAGAUACCAGCCGAAAGGCCCUUGGCAGCUAAUgguaUaUUCUgcugaugagcccaaauaggacgaaacgc
gcu
>Theo-5
ggcgaaagccggcgcguccuggauuccacUGUUGAUACCAGCCGAAAGGCCCUUGGCAGCACCAgguacaAACUgcugaugagucccaaauaggacgaaacgc
gcu
>Theo-6
gggcgaaagccggcgcguccuggauuccacUAAGUAUACCAGCCGAAAGGCCCUUGGCAGACUACgguacaACUUgcugaugagucccaaauaggacgaaacg
cgcu
>Theo-7
gggcugucaccggaugugcuuuccggucugaugaguccguguugcugAUACCAGCAUCGUCUUGAUGCCCUUGGCAGcaguggacgaggacgaaacagccc

p-AF aptazymes

>*p*-AF-1
gggcgaaagccggcgcguccuggauuccacUUUUCAUGUCCCUACCAUACGGGAUUGCCCAGCUUCGGCUGCCAUGCCGGCCAAACGGUAACCGGCCUACGCA
AACgguacaCCGGgcugaugagucccaaauaggacgaaacgcgcu
>*p*-AF-2
gggcgaaagccggcgcguccuggauuccacCAAGCAUGUCCCUACCAUACGGGAUUGCCCAGCUUCGGCUGCCAUGCCGGCCAAACGGUAACCGGCCUACGGG
AGGgguacaCAACgcugaugagucccaaauaggacgaaacgcgcu

Fig. S4. Ribozyme (**A**) and aptazyme (**B**) sequences. Stems I, II, and III are labeled consistently. Within each class of ribozyme or aptazyme, positions that were varied are colored in the primary sequences and secondary structure cartoons. Target secondary structures for the ribozymes are shown below each sequence in bracket form. See Table S4 for description of the aptazyme target secondary structures.

Table S3. Ribozyme and aptazyme *in vitro* cleavage rates at 30˚C.

Ribozyme	Length (nts)	k_{obs-} (min^{-1})		Reference	Change compared to published version
S. mansoni	82	1.28	± 0.03	(*18*)	
ASBV-1	80	3.64	± 0.12	(*48*)	engineered to cleave in *cis*
ASBV-2	79	1.74	± 0.27	(*48*)	engineered to cleave in *cis*
ASBV-3	80	0.06	± 0.02	(*48*)	engineered to cleave in *cis*
vLTSV-1	61	0.28	± 0.11	(*44*)	Stem III of sLTSV+ extended
vLTSV-2	60	0.08	± 0.02	(*44*)	Stem I and loop II variant of sLTSV+
sTRSV-1	52	0.60	± 0.36	(*44*)	Stem III of sTRSV+PL1 extended
sTRSV-2	62	0.31	± 0.07	(*44*)	Stem III of sTRSV+PL2 extended
sTRSV-3	56	0.10	± 0.05	(*44*)	Stem III of sTRSV+PL1&PL2 extended
sTRSV-4	54	<0.005	±	(*44*)	Stem II/Loop II variant of sTRSV+; Stem III extended
PLMVd	58	0.57	± 0.16	(*44*)	Stem III of PLMVd+ extended
HH2	71	<0.005	±	(*49*)	Stem I of HH2 extended

k_{obs-} measured in 1 mM Mg^{2+}, 0.5 mM EDTA, 50 mM Tris-HCl, pH 7.5

Theophylline aptazyme	Length (nts)	k_{obs-} (min^{-1})		k_{obs+} (min^{-1})		k_{obs+} / k_{obs-}	Reference	Designation in reference
Theo-1	107	0.07	± 0.04	0.38	± 0.14	5.4	(*18*)	VI-1
Theo-2	107	0.09	± 0.03	0.38	± 0.09	4.1	(*18*)	VI-2
Theo-3	107	0.18	± 0.08	0.30	± 0.13	1.7	(*18*)	VIII-3
Theo-4	106	0.010	± 0.003	0.14	± 0.06	14.2	(*18*)	VIII-5
Theo-5	106	0.016	± 0.005	0.31	± 0.08	19.3	(*18*)	IV-3
Theo-6	107	0.08	± 0.05	0.29	± 0.24	3.6	(*18*)	IV-5
Theo-7	101	0.08	± 0.08	0.11	± 0.07	1.5	(*16*)	L2BulgeOff1

k_{obs-} measured in 1 mM Mg^{2+}, 0.05 mM EDTA, 50 mM Tris-HCl, pH 7.5

k_{obs+} measured in 1 mM Mg2+, 0.05 mM EDTA, 50 mM Tris-HCl, pH 7.5 with 3 mM theophylline

p-AF aptazyme	Length (nts)	k_{obs-} (min^{-1})		k_{obs+} (min^{-1})		k_{obs+} / k_{obs-}	Reference	Designation in reference
p-AF-1	148	0.035	± 0.003	0.081	± 0.003	2.3	*This paper*	*p*-AF-1
p-AF-2	148	0.107	± 0.012	0.51	± 0.04	6.3	*This paper*	*p*-AF-2

k_{obs-} measured in 1 mM Mg^{2+}, 0.05 mM EDTA, 50 mM Tris-HCl, pH 7.5

k_{obs+} measured in 1 mM Mg2+, 0.05 mM EDTA, 50 mM Tris-HCl, pH 7.5 with 5 mM *p*-AF

A rREDs programming RFP expression

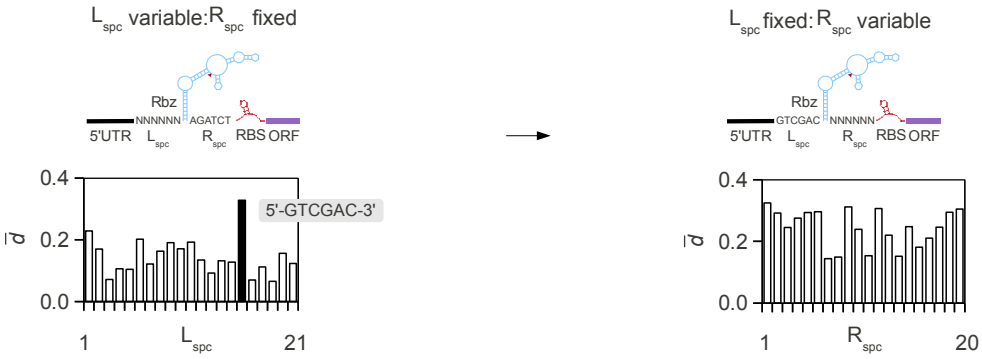

L_{spc}	sequence	$\bar{d}$	Z	L_{spc}	sequence	$\bar{d}$	Z
1	GACGTC	0.23	0.34	12	TGGCCA	0.13	-0.18
2	CTTAAG	0.17	0.38	13	CTGCAG	0.09	-0.86
3	CCTAGG	0.07	-1.21	14	GAGCTC	0.13	-0.22
4	TGATCA	0.11	-0.64	15	CCGCGG	0.13	-0.29
5	TGTACA	0.10	-0.68	16	GTCGAC	0.33	2.96
6	CGGCCG	0.20	0.91	17	AGTACT	0.07	-1.24
7	GAATTC	0.12	-0.40	18	TACGTA	0.11	-0.55
8	GATATC	0.16	0.27	19	ACTAGT	0.07	-1.31
9	CAATTG	0.19	0.73	20	AGGCCT	0.16	0.17
10	CATATG	0.17	0.40	21	TCTAGA	0.13	-0.36
11	GCTAGC	0.19	0.75				

R_{spc}	sequence	$\bar{d}$	Z	R_{spc}	sequence	$\bar{d}$	Z
1	GACGTC	0.32	1.22	11	GCTAGC	0.15	-1.53
2	CTTAAG	0.29	0.73	12	TGGCCA	0.31	1.06
3	CCTAGG	0.25	0.09	13	CTGCAG	0.22	-0.40
4	TGATCA	0.28	0.57	14	GAGCTC	0.15	-1.53
5	TGTACA	0.29	0.73	15	CCGCGG	0.25	0.09
6	CGGCCG	0.3	0.90	16	AGTACT	0.18	-1.04
7	GAATTC	0.14	-1.69	17	TACGTA	0.21	-0.56
8	GATATC	0.15	-1.53	18	ACTAGT	0.25	0.09
9	CAATTG	0.31	1.06	19	AGGCCT	0.29	0.73
10	CATATG	0.24	-0.07	20	TCTAGA	0.31	1.06

B rREDs programming papABC expression

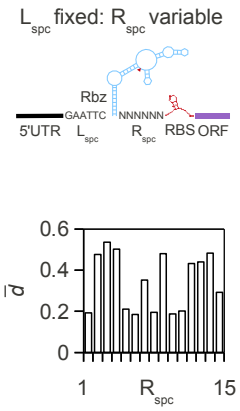

R_{spc}	sequence	$\bar{d}$	Z	R_{spc}	sequence	$\bar{d}$	Z
1	GGTACC	0.19	-1.09	11	GCTAGC	0.2	-1.02
2	ACCGGT	0.48	0.98	12	ATGCAT	0.43	0.62
3	TGATCA	0.54	1.40	13	TACGTA	0.44	0.69
4	TGTACA	0.5	1.12	14	AGGCCT	0.48	0.98
5	TTCGAA	0.21	-0.95	15	TCTAGA	0.29	-0.38
6	GTATAC	0.18	-1.17				
7	ATCGAT	0.35	0.05				
8	GATATC	0.19	-1.09				
9	AAGCTT	0.48	0.98				
10	GGTACC	0.19	-1.09				

Fig. S5. Transcript design. (**A**) Mean normalized distance scores ($\bar{d}$) for sets of rRED transcripts designed to program RFP expression are plotted for each of 21 L_{spc} and 20 R_{spc} sequences. The effect of fixing L_{spc} as GTCGAC (highest $\bar{d}$) and varying R_{spc} is illustrated at right. (**B**) $\bar{d}$ for sets of rRED transcripts designed to program papABC expression is plotted for each of 15 L_{spc} sequences. *Z* scores give the number of standard deviations that each $\bar{d}$ is from the mean observed for the specified L_{spc} or R_{spc} library sequence variants.

Table S4. Calculated ribozyme and aptazyme co-transcriptional folding rates.

rREDs programming RFP expression

name	k_{fold} (sec^{-1})		
rRED0-pPro-ref	0.000	±	0.000
rRED0-T7-ref	0.000	±	0.000
rRED1	0.106	±	0.005
rRED2	0.126	±	0.048
rRED3	0.095	±	0.012
rRED4	0.000	±	0.000
rRED5	0.000	±	0.000
rRED6	0.196	±	0.095
rRED7	0.000	±	0.000
rRED8	0.050	±	0.012
rRED9	0.000	±	0.000
rRED10	0.000	±	0.000
rRED11	0.000	±	0.000
rRED12	0.000	±	0.000
rRED13	0.052	±	0.008

aREDs programming RFP expression

name	k_{fold} (sec^{-1})			distinct structures[a]
aRED1	0.016	±	0.002	3
aRED2	0.000	±	0.000	1
aRED3	0.000	±	0.000	1
aRED4	0.000	±	0.000	1
aRED5	0.016	±	0.002	2
aRED6	0.000	±	0.000	1
aRED7	0.013	±	0.0003	2
aRED8	0.000	±	0.000	4
aRED9	0.012	±	0.001	4

rREDs programming papABC expression

name	k_{fold} (sec^{-1})		
rRED14-lac-ref	0.000	±	0.00
rRED15	0.089	±	0.02
rRED16	0.076	±	0.02
rRED17	1.320	±	0.31

[a] number of target secondary structures as predicted from minimal free energy folding of the aptazyme (i.e., not in the context of the rRED transcript)

Individual theophylline aptazyme molecules have been observed to interconvert between multiple structural conformations before ligand-binding and catalysis (*50*). All of the theophylline and *p*-AF aptazymes in our study exhibited self-cleavage activity in the presence and absence of ligand following thermal denaturation and annealing (Methods). We took the ensemble of distinct secondary structures predicted from kinetic secondary structure renaturation simulations as approximations of the target secondary structures for the purposes of calculating co-transcriptional aptazyme folding rates (k_{fold}). Briefly, the ensemble of target structures was taken as the distinct structures resulting from 100, 1 minute renaturation simulations with the kinefold_long_static binary (*22*) initiated with random seeds, helix minimum free energy = 6.346 kcal/mol and no pseudoknots or entanglements.

Table S5. Comparing minimal free energy and co-transcriptional kinetic folding.

L_{spc} = GTCGAC, $\bar{d}$ = 0.33			L_{spc} = TCTAGA, $\bar{d}$ = 0.13		L_{spc} = ACTAGT, $\bar{d}$ = 0.07	
rRED	**MFE target ?**	**k_{fold} > 0 ?**	**MFE target ?**	**k_{fold} > 0 ?**	**MFE target ?**	**k_{fold} > 0 ?**
1	yes	yes	yes	yes	yes	yes
2	no	yes	no	yes	no	yes
3	yes	yes	yes	yes	yes	yes
4	yes	no	yes	no	yes	no
6	no	yes	no	yes	no	yes
7	no	no	no	no	no	no
8	yes	yes	yes	yes	yes	yes
9	yes	yes	yes	no	yes	no
10	no	yes	no	no	no	no
11	no	no	no	no	no	no

MFE target = 'yes' indicates that the global minimal free energy secondary structure predicted for the rRED U_{ppp} transcript (Fig. 1B) has a ribozyme folded into the target secondary structure. k_{fold} > 0 = 'yes' indicates that the ribozyme is predicted to fold into the target secondary structure by co-transcriptional kinetic folding simulations (main text). Differences in MFE and kinetic folding predictions are highlighted in red.

The L_{spc}s shown correspond to those producing the largest, median and smallest mean normalized distance scores ($\bar{d}$) (main text, Fig. 2). Global MFE structures were determined for the U_{ppp} transcripts using Vienna RNAfold with default parameters (*51*). k_{fold} was determined with co-transcriptional kinetic folding simulations as described in the Methods. We note that there was very little agreement between predicted and observed γ_{rel} for rREDs programming RFP expression if MFE calculations were used to determine which device transcripts were expected to fold into the target structures (relative rmsd = 120%, see main text).

A rRED0-pPro, rRED13

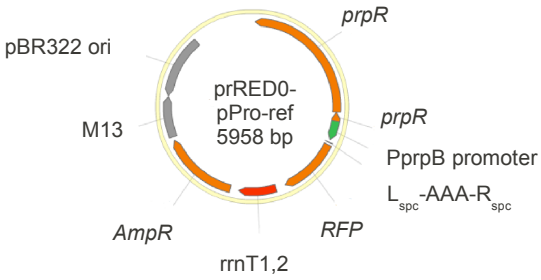

Promoter-ORF

pPro promoter 5'UTR L_{spc} R_{spc} RBS

5' end of DsRed (RFP)

```
5'CGCAGTAGATTCATCTTTAAGGGGCGATTTTTTGTTTT
AAACGTGTTTCATAAATGTTGCAATGAAACAGGGTGATTC
GTTTCATGAAACGTTAGCTGACACGTTTTTTTTTCCCTTA
ATCGCGCTTATTCATAACAGAAATGACTGTAATTACCTGT
TTTTAAATCTCATTGTATTTAATTTTCTCGCTGCCTCTTT
GCCTGGCATAGCCTTTGCTTTACGACGACAGGCACCCGAA
CTCTCTAGAAAAAGATCTGAAAGAGGAGAAATACTAGATG
GCTTCCTCCGAAGACGTTATCAAAGAGTTCATGCGTTTCA
AAGTTCGTATGGAAGGTTCCGTTAACGGTCACGAGTTCGA
AATCGAAGGTGAAGGTGAAGGTCGTCCGTACGAAGGTACC
CAGACCGCTAAACTGAAAGTTACCAAAGGTGGTCCGCTGC
CGTTCGCTTGGGACATCCTGTCCCCGCAGTTCCAGTACGG
TTCCAAAGCTTACGTTAAACACCCGGCTGACATCCCGGAC
TACCTGAAACTGTCCTTCCCGGAAGGTTTCAAATGGGAAC
GTGTTATGAAC...3'
```

B rRED2-rRED12, aRED1-aRED9

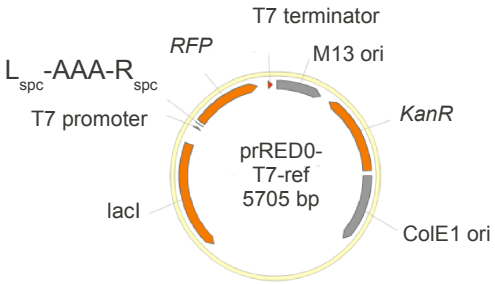

Promoter-ORF

T7 promoter 5'UTR L_{spc} R_{spc} RBS

5' end of DsRed (RFP)

```
5'GTCTAATACGACTCACTATAGGGACGACGACAGGCACC
CGAACTCTCTAGAAAAAGATCTGAAAGAGGAGAAATACTA
GATGGCTTCCTCCGAAGACGTTATCAAAGAGTTCATGCGT
TTCAAAGTTCGTATGGAAGGTTCCGTTAACGGTCACGAGT
TCGAAATCGAAGGTGAAGGTGAAGGTCGTCCGTACGAAGG
TACCCAGACCGCTAAACTGAAAGTTACCAAAGGTGGTCCG
CTGCCGTTCGCTTGGGACATCCTGTCCCCGCAGTTCCAGT
ACGGTTCCAAAGCTTACGTTAAACACCCGGCTGACATCCC
GGACTACCTGAAACTGTCCTTCCCGGAAGGTTTCAAATGG
GAACGTGTTATGAAC...3'
```

C rRED14-rRED17

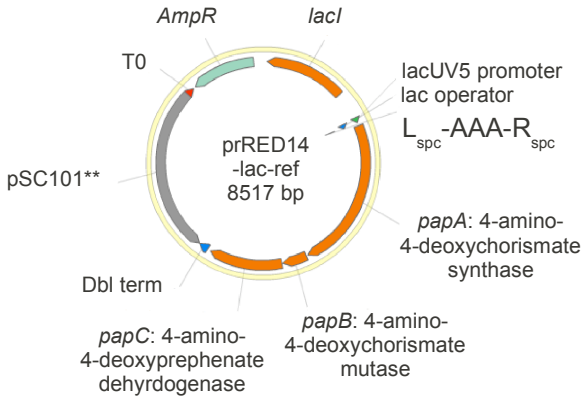

Promoter-1st ORF

lac promoter 5'UTR L_{spc} R_{spc} RBS

5' end of papA: 4-amino-4-deoxychorismate synthase

```
5'ATCGTTTAGGCACCCCAGGCTTTACACTTTATGCTTCC
GGCTCGTATAATGTGTGGAATTGTGAGCGGATAACAATTT
CAGAATTCAAATGTACAGATTCACACACAGGAAACAGCTA
TGCGCACGCTTCTGATCGACAACTACGACTCGTTCACCCA
CAACCTGTTCCAGTACATCGGCGAGGCCACCGGGCAGCCC
CCCGTCGTCGTGCCCAACGACGCCGACTGGTCGCGGCTGC
CCCTCGAGGACTTCGACGCGATCGTCGTGTCCCCGGGCCC
CGGCAGCCCCGACCGGGAACGGGACTTCGGGATCAGCCGC
CGGGCGATCACCGACAGCGGCCTGCCCGTCCTCGGCGTCT
GCCTCGGCCACCAGGGCATCGCCCAGCTCTTCGGCGGAAC
CGTCGGCC...3'
```

Fig. S6. Plasmids for expression device construction. (**A**) Plasmid map and region between promoter and 5' end of ORF for rRED0-pPro-ref and rRED13. (**B**) rRED2-12 and aRED1-9. (**C**) rRED14-lac-ref-rRED17. Reference device sequences are shown at right.

Table S6. Summary of component characteristics.

Design variable / parameter	Component(s)	Value (units)	Characterized	Method
$k_{init,\ txn}$		**(s^{-1})**		
	PprpB promoter	0.12	*in vivo*	Reported (*37*)
	pT7 promoter	0.28 ± 0.03	*in vivo*	Relative activity measurements (*14*)
	lacUV5 promoter	0.3	*in vivo*	Reported (*37*)
k_{pol}		**(nt s^{-1})**		
	T7 RNA polymerase	97	*in vivo*	Reported (*38,39*)
	E. coli RNA polymerase	25	*in vivo*	Reported (*38,39*)
ORF		**nts**		
	RFP	678	partsregistry.org	N.A.
	papABC operon	3399	(24)	N.A.
$k_{init,\ trans}$		**t (s)**		
	'strong' RBS sequence	2	*in vivo* / *in silico*	Reported (*41,42*)
k_{trans}		**(nt s^{-1})**		
	E. coli translation machinery	21	*in vivo*	Reported (*41,42*)
k_{fold}		**(s^{-1})**		
	rREDs 1-17	Table S4	*in silico*	Kinetic folding simulations
	aREDs 1-9	Table S4	*in silico*	Kinetic folding simulations
k_{obs-}		**(min^{-1})**		
	S. mansoni	Table S3	*in vitro*	Self-cleavage assays
	ASBV-1, 2, 3	Table S3	*in vitro*	Self-cleavage assays
	vLTSV-1, 2	Table S3	*in vitro*	Self-cleavage assays
	PLMVd	Table S3	*in vitro*	Self-cleavage assays
	sTRSV-1, 2, 3, 4	Table S3	*in vitro*	Self-cleavage assays
	HH2	Table S3	*in vitro*	Self-cleavage assays
	Theo-1, 2, 3, 4, 5, 6, 7	Table S3	*in vitro*	Self-cleavage assays
	p-AF-1, 2	Table S3	*in vitro*	Self-cleavage assays
k_{obs+}		**(min^{-1})**		
	Theo-1, 2, 3, 4, 5, 6, 7	Table S3	*in vitro*	Self-cleavage assays
	p-AF-1, 2	Table S3	*in vitro*	Self-cleavage assays
$RNA_{t1/2}$		**(min)**		
	rRED0-pPro-ref mRNA	1.2 ± 0.1	*in vivo*	RNA degradation qPCR assays
	rRED14-lac-ref mRNA	4.7 ± 0.6	*in vivo*	RNA degradation qPCR assays
$Protein_{t1/2}$		**(hrs)**		
	RFP	72	*in vivo*	Reported (*47*)
	papABC	10	*in vivo*	Reported (*47*)

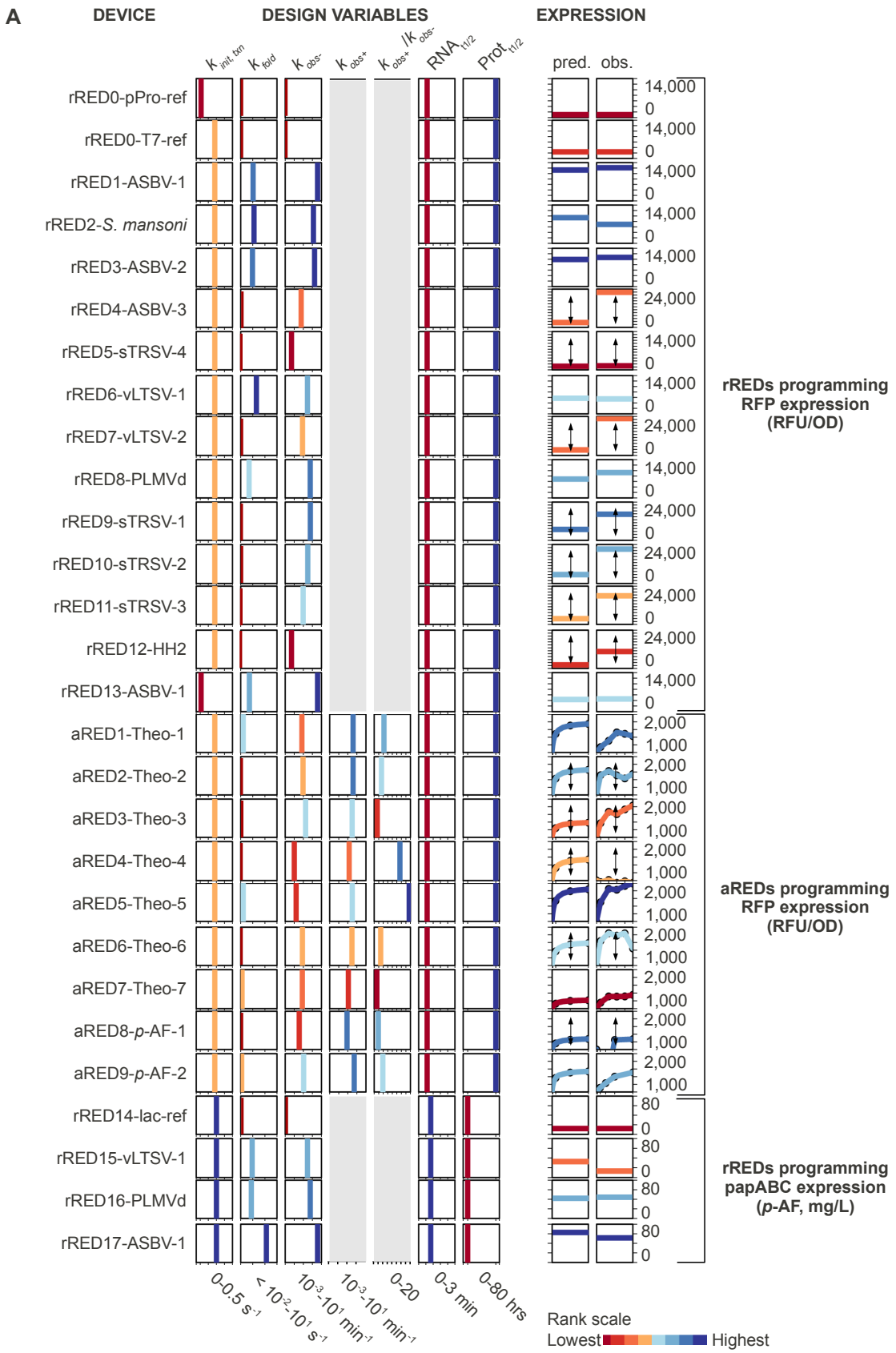

Fig. S7. rREDs and aREDs with programmable functions. (**A**) Selected design variables (left), predicted and measured expression levels (right), as in Fig. 3. Expression from devices with $k_{fold} < 0$ (↕) is not expected to fall within the domain of the mechanistic model.

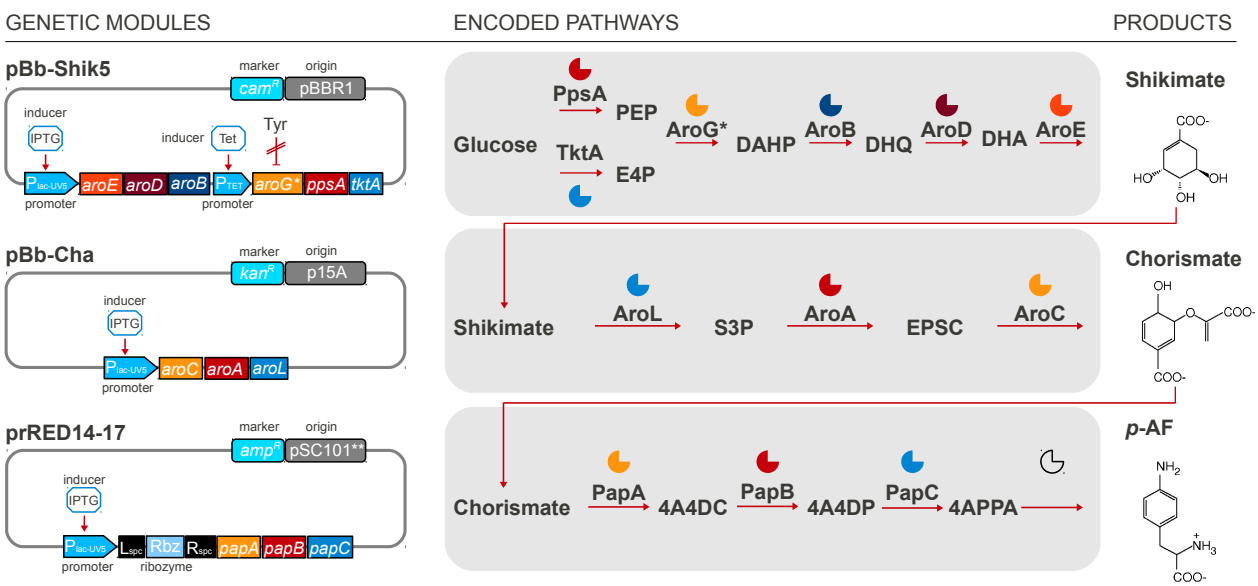

ENZYMES		CHEMICAL INTERMEDIATES	
PpsA	phosphoenolpyruvate synthase	**PEP**	phosphoenolpyruvate
TktA	transketolase A	**E4P**	erythrose-4-phosphate
AroG*	DAHP synthase (* feedback insensitive)	**DAHP**	3-deoxy-*D*-arabino-heptulosonate
AroB	DHQ synthase	**DHQ**	dehydroquinate
AroD	DHQ dehydratase	**DHS**	dehydroshikimate
AroE	shikimate dehydrogenase		
AroL	shikimate kinase	**S3P**	shikimate-3-phosphate
AroA	EPSP synthase	**EPSP**	5-enolpyruvoylshikimate
AroC	chorismate synthase		
PapA	4-amino-4-deoxychorismate synthase	**4A4DC**	4-amino-4-deoxychorismate
PapB	4-amino-deoxychorismate mutase	**4A4DP**	4-amino-4-deoxyprephenate
PapC	4-amino-4-deoxyprephenate dehydrogenase	**4APPA**	4-aminophenylpyruvic acid

Fig. S8. *E. coli* platform for high-titer, rRED-programmed, *p*-AF production. Three genetic modules were engineered to encode the biocatalytic pathways for converting glucose to shikimate (pBb-Shik5), shikimate to chorismate (pBb-Cha) and chorismate to *p*-AF (prRED14-17, encoding rREDs 14, 15, 16 and 17, also see Fig. S6 and Materials and Methods). Colors indicate the encoded gene products and the corresponding pathway enzymes.

Table S7. Summary of rRED and aRED expression.

rREDs expressing RFP in *E. coli* BL21

Expression Device	Ribozyme	Promoter	Predicted (RFU/OD)		Measured (RFU/OD)		Ribozyme $k_{fold} > 0$
rRED0-pPro	none	PprpB	1000	± 70	1000	± 70	N.A.
rRED0-T7	none	T7	2410	± 150	2410	± 150	N.A.
rRED1	ASBV-1	T7	11280	± 440	12120	± 820	yes
rRED2	*S. mansoni*	T7	9390	± 400	6940	± 430	yes
rRED3	ASBV-2	T7	9920	± 400	10680	± 480	yes
rRED4	ASBV-3	T7	3320	± 160	23880	± 870	no
rRED5	sTRSV-4	T7	2400	± 90	2680	± 150	no
rRED6	vLTSV-1	T7	5700	± 450	5470	± 270	yes
rRED7	vLTSV-2	T7	3660	± 180	24560	± 360	no
rRED8	PLMVd	T7	6880	± 410	9250	± 300	yes
rRED9	sTRSV-1	T7	7420	± 710	17710	± 750	no
rRED10	sTRSV-2	T7	5920	± 330	22940	± 1010	no
rRED11	sTRSV-3	T7	3850	± 290	1940	± 600	no
rRED12	HH2	T7	2410	± 90	11500	± 430	no
rRED13	ASBV-1	PprpB	4340	± 420	4530	± 320	yes

Expression in LB at 30˚C for 18-24 hours (see Methods). rRED0-pPro and rRED0-T7 are reference devices; accordingly predicted γ_{rel} equals measured γ_{rel} for those devices. ± s.d. is shown.

aREDs expressing RFP in *E. coli* BL21

Expression device	Aptazyme	Promoter	Predicted (RFU/OD)		Measured (RFU/OD)		Ribozyme $k_{fold} > 0$
aRED1	Theo-1	T7	1750	± 350	1550	± 80	yes
aRED2	Theo-2	T7	1690	± 260	1480	± 130	no
aRED3	Theo-3	T7	1410	± 300	1850	± 60	no
aRED4	Theo-4	T7	1570	± 250	980	± 100	no
aRED5	Theo-5	T7	1890	± 260	1930	± 110	yes
aRED6	Theo-6	T7	1640	± 400	1930	± 220	no
aRED7	Theo-7	T7	1210	± 250	1310	± 110	yes
aRED8	*p*-AF-1	T7	1310	± 100	1270	± 40	no
aRED9	*p*-AF-2	T7	1570	± 140	1500	± 10	yes

Expression in LB at 30˚C for 18-24 hours (see Methods) with ligand added directly to the media. For aRED1-7, measured γ_{rel} corresponds to the maximum RFP expression observed (7mM theophylline) compared to the reference (no ligand). For aRED8 and aRED9, measured γ_{rel} corresponds to the maximum RFP expression observed (10 mM *p*-AF) compared to the reference (no ligand). ± s.d. is shown.

rREDs expressing papABC to produce *p*-AF in *E. coli* MG1655-derived chorismate overproducing strain

Expression device	Ribozyme	Promoter	Predicted *p*-AF (mg/L)		Measured *p*-AF (mg/L)		Ribozyme $k_{fold} > 0$
rRED14-lac	none	lac	12.1	± 3.0	12.1	± 3.0	N.A.
rRED15	vLTSV-1	lac	45.7	± 12.9	13.3	± 1.7	yes
rRED16	PLMVd	lac	53.7	± 14.5	44.3	± 0.5	yes
rRED17	ASBV-1	lac	65.1	± 17.5	51.3	± 0.4	yes

Expression in MOPS M9 + 0.5% glucose at 30˚C for 30 hours (see Methods). rRED14-lac is the reference device; accordingly, predicted *p*-AF production equals measured *p*-AF production for that device. Corresponding predicted γ_{rel} values for rRED15, rRED16 and rRED17 are 3.8 ± 0.7, 4.4 ± 0.7, and 5.4 ± 0.8, respectively. ± s.d. is shown.

Parameter values presented in Tables S3, S4 and S6 were employed to generate model-derived predictions of rRED and aRED γ_{rel}. By definition, for reference devices (denoted with 'ref'), the predicted γ_{rel} equals measured γ_{rel}. Measured γ_{rel} is expected to match predicted γ_{rel} only for those expression devices designed such that the ribozyme or aptazyme folds into the target secondary structure (i.e., $k_{fold} > 0$). The mean k_{fold} for rREDs with $k_{fold} > 0$ (0.104 ± 0.025 s^{-1}) was assigned to rREDs with $k_{fold} < 0$ and the mean k_{fold} for aREDs with $k_{fold} > 0$ (0.014 ± 0.001 s^{-1}) was assigned to aREDs with $k_{fold} < 0$ to calculate predicted γ_{rel} values in those cases.

Expression device sequences

rRED and aRED sequences are shown in FASTA format with coloring as indicated for the reference device sequences in Fig. S6. The order is the same as in Fig. S7.0

>rRED0-pPro-ref
CGCAGTAGATTCATCTTTAAGGGGCGATTTTTTGTTTTAAACGTGTTTCATAAATGTTGCAATGAAACAGGGTGATTCGTTT
CATGAAACGTTAGCTGACACGTTTTTTTTTCCCTTAATCGCGCTTATTCATAACAGAAATGACTGTAATTACCTGTTTTTAA
ATCTCATTGTATTTAATTTTCTCGCTGCCTCTTTGCCTGGCATAGCCTTTGCTTTACGACGACAGGCACCCGAACTCTCTAG
AAAAAGATCTGAAAGAGGAGAAATACTAGATGGCTTCCTCCGAAGACGTTATCAAAGAGTTCATGCGTTTCAAAGTTCGTAT
GGAAGGTTCCGTTAACGGTCACGAGTTCGAAATCGAAGGTGAAGGTGAAGGTCGTCCGTACGAAGGTACCCAGACCGCTAAA
CTGAAAGTTACCAAAGGTGGTCCGCTGCCGTTCGCTTGGGACATCCTGTCCCCGCAGTTCCAGTACGGTTCCAAAGCTTACG
TTAAACACCCGGCTGACATCCCGGACTACCTGAAACTGTCCTTCCCGGAAGGTTTCAAATGGGAACGTGTTATGAAC...
>rRED0-T7-ref
GTCTAATACGACTCACTATAGGGACGACGACAGGCACCCGAACTCTCTAGAAAAGATCTGAAAGAGGAGAAATACTAGATG
GCTTCCTCCGAAGACGTTATCAAAGAGTTCATGCGTTTCAAAGTTCGTATGGAAGGTTCCGTTAACGGTCACGAGTTCGAAA
TCGAAGGTGAAGGTGAAGGTCGTCCGTACGAAGGTACCCAGACCGCTAAACTGAAAGTTACCAAAGGTGGTCCGCTGCCGTT
CGCTTGGGACATCCTGTCCCCGCAGTTCCAGTACGGTTCCAAAGCTTACGTTAAACACCCGGCTGACATCCCGGACTACCTG
AAACTGTCCTTCCCGGAAGGTTTCAAATGGGAACGTGTTATGAAC...
>rRED1-ASBV-1
GTCTAATACGACTCACTATAGGGACGACGACAGGCACCCGAACTCTCTAGAGGGACGGGCCATCATCTATCCCTGAAGAGAC
GAAGGCTTCGGCCAAGTCGAAACGGAAACGTCGGATAGTCGCCCGTCCCAGATCTGAAAGAGGAGAAATACTAGATGGCTTC
CTCCGAAGACGTTATCAAAGAGTTCATGCGTTTCAAAGTTCGTATGGAAGGTTCCGTTAACGGTCACGAGTTCGAAATCGAA
GGTGAAGGTGAAGGTCGTCCGTACGAAGGTACCCAGACCGCTAAACTGAAAGTTACCAAAGGTGGTCCGCTGCCGTTCGCTT
GGGACATCCTGTCCCCGCAGTTCCAGTACGGTTCCAAAGCTTACGTTAAACACCCGGCTGACATCCCGGACTACCTGAAACT
GTCCTTCCCGGAAGGTTTCAAATGGGAACGTGTTATGAAC...
>rRED2-*S. mansoni*
GTCTAATACGACTCACTATAGGGACGACGACAGGCACCCGAACTCTCTAGAGGGCGAAAGCCGGCGCGTCCTGGATTCCACT
GCTTCGGCAGGTACATCCAGCTGATGAGTCCCAAATAGGACGAAACGCGCTAGATCTGAAAGAGGAGAAATACTAGATGGCT
TCCTCCGAAGACGTTATCAAAGAGTTCATGCGTTTCAAAGTTCGTATGGAAGGTTCCGTTAACGGTCACGAGTTCGAAATCG
AAGGTGAAGGTGAAGGTCGTCCGTACGAAGGTACCCAGACCGCTAAACTGAAAGTTACCAAAGGTGGTCCGCTGCCGTTCGC
TTGGGACATCCTGTCCCCGCAGTTCCAGTACGGTTCCAAAGCTTACGTTAAACACCCGGCTGACATCCCGGACTACCTGAAA
CTGTCCTTCCCGGAAGGTTTCAAATGGGAACGTGTTATGAAC...
>rRED3-ASBV-2
GTCTAATACGACTCACTATAGGGACGACGACAGGCACCCGAACTCTCTAGAGGGACGGGCCATCATCTATCCCTGAAGAGAC
GAAGGCTTCGGCCAGTCGAAACGGAAACGTCGGATAGTCGCCCGTCCCAGATCTGAAAGAGGAGAAATACTAGATGGCTTCC
TCCGAAGACGTTATCAAAGAGTTCATGCGTTTCAAAGTTCGTATGGAAGGTTCCGTTAACGGTCACGAGTTCGAAATCGAAG
GTGAAGGTGAAGGTCGTCCGTACGAAGGTACCCAGACCGCTAAACTGAAAGTTACCAAAGGTGGTCCGCTGCCGTTCGCTTG
GGACATCCTGTCCCCGCAGTTCCAGTACGGTTCCAAAGCTTACGTTAAACACCCGGCTGACATCCCGGACTACCTGAAACTG
TCCTTCCCGGAAGGTTTCAAATGGGAACGTGTTATGAAC...
>rRED4-ASBV-3
GTCTAATACGACTCACTATAGGGACGACGACAGGCACCCGAACTCTCTAGAGGGACGGGCCATCATCTATCCCTGAAGAGAC
GAAGGCTTCGGCCTCGTCGAAACGGAAACGTGGGATAGTCGCCCGTCCCAGATCTGAAAGAGGAGAAATACTAGATGGCTTC
CTCCGAAGACGTTATCAAAGAGTTCATGCGTTTCAAAGTTCGTATGGAAGGTTCCGTTAACGGTCACGAGTTCGAAATCGAA
GGTGAAGGTGAAGGTCGTCCGTACGAAGGTACCCAGACCGCTAAACTGAAAGTTACCAAAGGTGGTCCGCTGCCGTTCGCTT
GGGACATCCTGTCCCCGCAGTTCCAGTACGGTTCCAAAGCTTACGTTAAACACCCGGCTGACATCCCGGACTACCTGAAACT
GTCCTTCCCGGAAGGTTTCAAATGGGAACGTGTTATGAAC...
>rRED5-sTRSV-4
GTCTAATACGACTCACTATAGGGACGACGACAGGCACCCGAACTCTCTAGAGGGCTGTCACCGGATGTGCTTTCCGGTCTGA
TGAGCCGGAGGACGAAACAGCCCAGATCTGAAAGAGGAGAAATACTAGATGGCTTCCTCCGAAGACGTTATCAAAGAGTTCA
TGCGTTTCAAAGTTCGTATGGAAGGTTCCGTTAACGGTCACGAGTTCGAAATCGAAGGTGAAGGTGAAGGTCGTCCGTACGA
AGGTACCCAGACCGCTAAACTGAAAGTTACCAAAGGTGGTCCGCTGCCGTTCGCTTGGGACATCCTGTCCCCGCAGTTCCAG
TACGGTTCCAAAGCTTACGTTAAACACCCGGCTGACATCCCGGACTACCTGAAACTGTCCTTCCCGGAAGGTTTCAAATGGG
AACGTGTTATGAAC...

>rRED6-vLTSV-1
GTCTAATACGACTCACTATAGGGACGACGACAGGCACCCGAACTCTCTAGAGGGTACGTCTGAGCGTGATACCCGCTCACTG
AAGATGGCCCGGTAGGGCCGAAACGTACCCAGATCTGAAAGAGGAGAAATACTAGATGGCTTCCTCCGAAGACGTTATCAAA
GAGTTCATGCGTTTCAAAGTTCGTATGGAAGGTTCCGTTAACGGTCACGAGTTCGAAATCGAAGGTGAAGGTGAAGGTCGTC
CGTACGAAGGTACCCAGACCGCTAAACTGAAAGTTACCAAAGGTGGTCCGCTGCCGTTCGCTTGGGACATCCTGTCCCCGCA
GTTCCAGTACGGTTCCAAAGCTTACGTTAAACACCCGGCTGACATCCCGGACTACCTGAAACTGTCCTTCCCGGAAGGTTTC
AAATGGGAACGTGTTATGAAC...
>rRED7-vLTSV-2
GTCTAATACGACTCACTATAGGGACGACGACAGGCACCCGAACTCTCTAGAGGGTACGTTGAGCGTGATACCCGCTCACTGA
AGATGGCCCGATAGGGCCGAAACGTACCCAGATCTGAAAGAGGAGAAATACTAGATGGCTTCCTCCGAAGACGTTATCAAAG
AGTTCATGCGTTTCAAAGTTCGTATGGAAGGTTCCGTTAACGGTCACGAGTTCGAAATCGAAGGTGAAGGTGAAGGTCGTCC
GTACGAAGGTACCCAGACCGCTAAACTGAAAGTTACCAAAGGTGGTCCGCTGCCGTTCGCTTGGGACATCCTGTCCCCGCAG
TTCCAGTACGGTTCCAAAGCTTACGTTAAACACCCGGCTGACATCCCGGACTACCTGAAACTGTCCTTCCCGGAAGGTTTCA
AATGGGAACGTGTTATGAAC...
>rRED8-PLMVd
GTCTAATACGACTCACTATAGGGACGACGACAGGCACCCGAACTCTCTAGAGGGAAGAGTCTGTGCTAAGCACACTGACGAG
TCTCTGAGATGAGACGAAACTCTTCCCAGATCTGAAAGAGGAGAAATACTAGATGGCTTCCTCCGAAGACGTTATCAAAGAG
TTCATGCGTTTCAAAGTTCGTATGGAAGGTTCCGTTAACGGTCACGAGTTCGAAATCGAAGGTGAAGGTGAAGGTCGTCCGT
ACGAAGGTACCCAGACCGCTAAACTGAAAGTTACCAAAGGTGGTCCGCTGCCGTTCGCTTGGGACATCCTGTCCCCGCAGTT
CCAGTACGGTTCCAAAGCTTACGTTAAACACCCGGCTGACATCCCGGACTACCTGAAACTGTCCTTCCCGGAAGGTTTCAAA
TGGGAACGTGTTATGAAC...
>rRED9-sTRSV-1
GTCTAATACGACTCACTATAGGGACGACGACAGGCACCCGAACTCTCTAGAGGGCCTGTCACCGGTAACCGGTCTGATGAGT
CCGTGAGGACGAAACAGGCCCAGATCTGAAAGAGGAGAAATACTAGATGGCTTCCTCCGAAGACGTTATCAAAGAGTTCATG
CGTTTCAAAGTTCGTATGGAAGGTTCCGTTAACGGTCACGAGTTCGAAATCGAAGGTGAAGGTGAAGGTCGTCCGTACGAAG
GTACCCAGACCGCTAAACTGAAAGTTACCAAAGGTGGTCCGCTGCCGTTCGCTTGGGACATCCTGTCCCCGCAGTTCCAGTA
CGGTTCCAAAGCTTACGTTAAACACCCGGCTGACATCCCGGACTACCTGAAACTGTCCTTCCCGGAAGGTTTCAAATGGGAA
CGTGTTATGAAC...
>rRED10-sTRSV-2
GTCTAATACGACTCACTATAGGGACGACGACAGGCACCCGAACTCTCTAGAGGGCCTGTCACCGGATGTGCTTTCCGGTCTG
ATGAGTCCCTGAAATGGGACGAAACAGGCCCAGATCTGAAAGAGGAGAAATACTAGATGGCTTCCTCCGAAGACGTTATCAA
AGAGTTCATGCGTTTCAAAGTTCGTATGGAAGGTTCCGTTAACGGTCACGAGTTCGAAATCGAAGGTGAAGGTGAAGGTCGT
CCGTACGAAGGTACCCAGACCGCTAAACTGAAAGTTACCAAAGGTGGTCCGCTGCCGTTCGCTTGGGACATCCTGTCCCCGC
AGTTCCAGTACGGTTCCAAAGCTTACGTTAAACACCCGGCTGACATCCCGGACTACCTGAAACTGTCCTTCCCGGAAGGTTT
CAAATGGGAACGTGTTATGAAC...
>rRED11-sTRSV-3
GTCTAATACGACTCACTATAGGGACGACGACAGGCACCCGAACTCTCTAGAGGGCCTGTCACCGGTAACCGGTCTGATGAGT
CCCTGAAATGGGACGAAACAGGCCCAGATCTGAAAGAGGAGAAATACTAGATGGCTTCCTCCGAAGACGTTATCAAAGAGTT
CATGCGTTTCAAAGTTCGTATGGAAGGTTCCGTTAACGGTCACGAGTTCGAAATCGAAGGTGAAGGTGAAGGTCGTCCGTAC
GAAGGTACCCAGACCGCTAAACTGAAAGTTACCAAAGGTGGTCCGCTGCCGTTCGCTTGGGACATCCTGTCCCCGCAGTTCC
AGTACGGTTCCAAAGCTTACGTTAAACACCCGGCTGACATCCCGGACTACCTGAAACTGTCCTTCCCGGAAGGTTTCAAATG
GGAACGTGTTATGAAC...
>rRED12-HH2
GTCTAATACGACTCACTATAGGGACGACGACAGGCACCCGAACTCTCTAGAGGGCGATGACCTGATGAGGCCGAAAGGCCGA
AAGGCCGAAACGTTCTCGCGAGAGAACGTCGTCGTCGCCCAGATCTGAAAGAGGAGAAATACTAGATGGCTTCCTCCGAAGA
CGTTATCAAAGAGTTCATGCGTTTCAAAGTTCGTATGGAAGGTTCCGTTAACGGTCACGAGTTCGAAATCGAAGGTGAAGGT
GAAGGTCGTCCGTACGAAGGTACCCAGACCGCTAAACTGAAAGTTACCAAAGGTGGTCCGCTGCCGTTCGCTTGGGACATCC
TGTCCCCGCAGTTCCAGTACGGTTCCAAAGCTTACGTTAAACACCCGGCTGACATCCCGGACTACCTGAAACTGTCCTTCCC
GGAAGGTTTCAAATGGGAACGTGTTATGAAC...
>rRED13-ASBV-1
CGCAGTAGATTCATCTTTAAGGGGCGATTTTTTGTTTTAAACGTGTTTCATAAATGTTGCAATGAAACAGGGTGATTCGTTT
CATGAAACGTTAGCTGACACGTTTTTTTTTCCCTTAATCGCGCTTATTCATAACAGAAATGACTGTAATTACCTGTTTTTAA
ATCTCATTGTATTTAATTTTCTCGCTGCCTCTTTGCCTGGCATAGCCTTTGCTTTACGACGACAGGCACCCGAACTCTCTAG
AGGGACGGGCCATCATCTATCCCTGAAGAGACGAAGGCTTCGGCCAAGTCGAAACGGAAACGTCGGATAGTCGCCCGTCCC
AGATCTGAAAGAGGAGAAATACTAGATGGCTTCCTCCGAAGACGTTATCAAAGAGTTCATGCGTTTCAAAGTTCGTATGGAA
GGTTCCGTTAACGGTCACGAGTTCGAAATCGAAGGTGAAGGTGAAGGTCGTCCGTACGAAGGTACCCAGACCGCTAAACTGA
AAGTTACCAAAGGTGGTCCGCTGCCGTTCGCTTGGGACATCCTGTCCCCGCAGTTCCAGTACGGTTCCAAAGCTTACGTTAA
ACACCCGGCTGACATCCCGGACTACCTGAAACTGTCCTTCCCGGAAGGTTTCAAATGGGAACGTGTTATGAAC...

>aRED1-Theo-1
GTCTAATACGACTCACTATAGGGACGACGACAGGCACCCGAACTCTCTAGAGGGCGAAAGCCGGCGCGTCCTGGATTCCACG
AGATATACCAGCCGAAAGGCCCTTGGCAGCTCCCGGAACAACCTGCTGACGAGTCCCAAATAGGACGAAACGCGCTAGATCT
GAAAGAGGAGAAATACTAGATGGCTTCCTCCGAAGACGTTATCAAAGAGTTCATGCGTTTCAAAGTTCGTATGGAAGGTTCC
GTTAACGGTCACGAGTTCGAAATCGAAGGTGAAGGTGAAGGTCGTCCGTACGAAGGTACCCAGACCGCTAAACTGAAAGTTA
CCAAAGGTGGTCCGCTGCCGTTCGCTTGGGACATCCTGTCCCCGCAGTTCCAGTACGGTTCCAAAGCTTACGTTAAACACCC
GGCTGACATCCCGGACTACCTGAAACTGTCCTTCCCGGAAGGTTTCAAATGGGAACGTGTTATGAAC...
>aRED2-Theo-2
GTCTAATACGACTCACTATAGGGACGACGACAGGCACCCGAACTCTCTAGAGGGCGAAAGCCGGCGCGTCCTGGATTCCACC
CGAGATACCAGCCGAAAGGCCCTTGGCAGCTCCCGGAACAACCTGCTGATGAGTCCCAAATAGGACGAAACGCGCTAGATCT
GAAAGAGGAGAAATACTAGATGGCTTCCTCCGAAGACGTTATCAAAGAGTTCATGCGTTTCAAAGTTCGTATGGAAGGTTCC
GTTAACGGTCACGAGTTCGAAATCGAAGGTGAAGGTGAAGGTCGTCCGTACGAAGGTACCCAGACCGCTAAACTGAAAGTTA
CCAAAGGTGGTCCGCTGCCGTTCGCTTGGGACATCCTGTCCCCGCAGTTCCAGTACGGTTCCAAAGCTTACGTTAAACACCC
GGCTGACATCCCGGACTACCTGAAACTGTCCTTCCCGGAAGGTTTCAAATGGGAACGTGTTATGAAC...
>aRED3-Theo-3
GTCTAATACGACTCACTATAGGGACGACGACAGGCACCCGAACTCTCTAGAGGGCGAAAGCCGGCGCGTCCTGGATTCCACA
TGTATACCAGCCGAAAGGCCCTTGGCAGACTTTGGTACATGAAGCTGATGAGTCCCCAAATAGGACGAAACGCGCTAGATCT
GAAAGAGGAGAAATACTAGATGGCTTCCTCCGAAGACGTTATCAAAGAGTTCATGCGTTTCAAAGTTCGTATGGAAGGTTCC
GTTAACGGTCACGAGTTCGAAATCGAAGGTGAAGGTGAAGGTCGTCCGTACGAAGGTACCCAGACCGCTAAACTGAAAGTTA
CCAAAGGTGGTCCGCTGCCGTTCGCTTGGGACATCCTGTCCCCGCAGTTCCAGTACGGTTCCAAAGCTTACGTTAAACACCC
GGCTGACATCCCGGACTACCTGAAACTGTCCTTCCCGGAAGGTTTCAAATGGGAACGTGTTATGAAC...
>aRED4-Theo-4
GTCTAATACGACTCACTATAGGGACGACGACAGGCACCCGAACTCTCTAGAGGGCGAAAGCCGGCGCGTCCTGGATTCCACA
ATAGATACCAGCCGAAAGGCCCTTGGCAGCTAATGGTATATTCTGCTGATGAGCCCAAATAGGACGAAACGCGCTAGATCTG
AAAGAGGAGAAATACTAGATGGCTTCCTCCGAAGACGTTATCAAAGAGTTCATGCGTTTCAAAGTTCGTATGGAAGGTTCCG
TTAACGGTCACGAGTTCGAAATCGAAGGTGAAGGTGAAGGTCGTCCGTACGAAGGTACCCAGACCGCTAAACTGAAAGTTAC
CAAAGGTGGTCCGCTGCCGTTCGCTTGGGACATCCTGTCCCCGCAGTTCCAGTACGGTTCCAAAGCTTACGTTAAACACCCG
GCTGACATCCCGGACTACCTGAAACTGTCCTTCCCGGAAGGTTTCAAATGGGAACGTGTTATGAAC...
>aRED5-Theo-5
GTCTAATACGACTCACTATAGGGACGACGACAGGCACCCGAACTCTCTAGAGGCGAAAGCCGGCGCGTCCTGGATTCCACTG
TTGATACCAGCCGAAAGGCCCTTGGCAGCACCAGGTACAAACTGCTGATGAGTCCCAAATAGGACGAAACGCGCTAGATCTG
AAAGAGGAGAAATACTAGATGGCTTCCTCCGAAGACGTTATCAAAGAGTTCATGCGTTTCAAAGTTCGTATGGAAGGTTCCG
TTAACGGTCACGAGTTCGAAATCGAAGGTGAAGGTGAAGGTCGTCCGTACGAAGGTACCCAGACCGCTAAACTGAAAGTTAC
CAAAGGTGGTCCGCTGCCGTTCGCTTGGGACATCCTGTCCCCGCAGTTCCAGTACGGTTCCAAAGCTTACGTTAAACACCCG
GCTGACATCCCGGACTACCTGAAACTGTCCTTCCCGGAAGGTTTCAAATGGGAACGTGTTATGAAC...
>aRED6-Theo-6
GTCTAATACGACTCACTATAGGGACGACGACAGGCACCCGAACTCTCTAGAGGGCGAAAGCCGGCGCGTCCTGGATTCCACT
AAGTATACCAGCCGAAAGGCCCTTGGCAGACTACGGTACAACTTGCTGATGAGTCCCAAATAGGACGAAACGCGCTAGATCT
GAAAGAGGAGAAATACTAGATGGCTTCCTCCGAAGACGTTATCAAAGAGTTCATGCGTTTCAAAGTTCGTATGGAAGGTTCC
GTTAACGGTCACGAGTTCGAAATCGAAGGTGAAGGTGAAGGTCGTCCGTACGAAGGTACCCAGACCGCTAAACTGAAAGTTA
CCAAAGGTGGTCCGCTGCCGTTCGCTTGGGACATCCTGTCCCCGCAGTTCCAGTACGGTTCCAAAGCTTACGTTAAACACCC
GGCTGACATCCCGGACTACCTGAAACTGTCCTTCCCGGAAGGTTTCAAATGGGAACGTGTTATGAAC...
>aRED7-Theo-7
GTCTAATACGACTCACTATAGGGACGACGACAGGCACCCGAACTCTCTAGAGGGCTGTCACCGGATGTGCTTTCCGGTCTGA
TGAGTCCGTGTTGCTGATACCAGCATCGTCTTGATGCCCTTGGCAGCAGTGGACGAGGACGAAACAGCCCAGATCTGAAAGA
GGAGAAATACTAGATGGCTTCCTCCGAAGACGTTATCAAAGAGTTCATGCGTTTCAAAGTTCGTATGGAAGGTTCCGTTAAC
GGTCACGAGTTCGAAATCGAAGGTGAAGGTGAAGGTCGTCCGTACGAAGGTACCCAGACCGCTAAACTGAAAGTTACCAAAG
GTGGTCCGCTGCCGTTCGCTTGGGACATCCTGTCCCCGCAGTTCCAGTACGGTTCCAAAGCTTACGTTAAACACCCGGCTGA
CATCCCGGACTACCTGAAACTGTCCTTCCCGGAAGGTTTCAAATGGGAACGTGTTATGAAC...
>aRED8-*p*-AF-1
GTCTAATACGACTCACTATAGGGACGACGACAGGCACCCGAACTCTCTAGAGGGCGAAAGCCGGCGCGTCCTGGATTCCACT
TTTCATGTCCCTACCATACGGGATTGCCCAGCTTCGGCTGCCATGCCGGCCAAACGGTAACCGGCCTACGCAAACGGTACAC
CGGGCTGATGAGTCCCAAATAGGACGAAACGCGCTAGATCTGAAAGAGGAGAAATACTAGATGGCTTCCTCCGAAGACGTTA
TCAAAGAGTTCATGCGTTTCAAAGTTCGTATGGAAGGTTCCGTTAACGGTCACGAGTTCGAAATCGAAGGTGAAGGTGAAGG
TCGTCCGTACGAAGGTACCCAGACCGCTAAACTGAAAGTTACCAAAGGTGGTCCGCTGCCGTTCGCTTGGGACATCCTGTCC
CCGCAGTTCCAGTACGGTTCCAAAGCTTACGTTAAACACCCGGCTGACATCCCGGACTACCTGAAACTGTCCTTCCCGGAAG
GTTTCAAATGGGAACGTGTTATGAAC...

>aRED9-*p*-AF-2
GTCTAATACGACTCACTATAGGGACGACGACAGGCACCCGAACTCTCTAGAGGGCGAAAGCCGGCGCGTCCTGGATTCCACC
AAGCATGTCCCTACCATACGGGATTGCCCAGCTTCGGCTGCCATGCCGGCCAAACGGTAACCGGCCTACGGGAGGGGTACAC
AACGCTGATGAGTCCCAAATAGGACGAAACGCGCTAGATCTGAAAGAGGAGAAATACTAGATGGCTTCCTCCGAAGACGTTA
TCAAAGAGTTCATGCGTTTCAAAGTTCGTATGGAAGGTTCCGTTAACGGTCACGAGTTCGAAATCGAAGGTGAAGGTGAAGG
TCGTCCGTACGAAGGTACCCAGACCGCTAAACTGAAAGTTACCAAAGGTGGTCCGCTGCCGTTCGCTTGGGACATCCTGTCC
CCGCAGTTCCAGTACGGTTCCAAAGCTTACGTTAAACACCCGGCTGACATCCCGGACTACCTGAAACTGTCCTTCCCGGAAG
GTTTCAAATGGGAACGTGTTATGAAC...
>rRED14-lac-ref
ATCGTTTAGGCACCCCAGGCTTTACACTTTATGCTTCCGGCTCGTATAATGTGTGGAATTGTGAGCGGATAACAATTTCAGA
ATTCAAATGTACAGATTCACACACAGGAAACAGCTATGCGCACGCTTCTGATCGACAACTACGACTCGTTCACCCACAACCT
GTTCCAGTACATCGGCGAGGCCACCGGGCAGCCCCCCGTCGTCGTGCCCAACGACGCCGACTGGTCGCGGCTGCCCCTCGAG
GACTTCGACGCGATCGTCGTGTCCCCGGGCCCCGGCAGCCCCGACCGGGAACGGGACTTCGGGATCAGCCGCCGGGCGATCA
CCGACAGCGGCCTGCCCGTCCTCGGCGTCTGCCTCGGCCACCAGGGCATCGCCCAGCTCTTCGGCGGAACCGTCGGCC...
>rRED15-vLTSV-1
ATCGTTTAGGCACCCCAGGCTTTACACTTTATGCTTCCGGCTCGTATAATGTGTGGAATTGTGAGCGGATAACAATTTCAGA
ATTCGGGTACGTCTGAGCGTGATACCCGCTCACTGAAGATGGCCCGGTAGGGCCGAAACGTACCCTGTACAGATTCACACAC
AGGAAACAGCTATGCGCACGCTTCTGATCGACAACTACGACTCGTTCACCCACAACCTGTTCCAGTACATCGGCGAGGCCAC
CGGGCAGCCCCCCGTCGTCGTGCCCAACGACGCCGACTGGTCGCGGCTGCCCCTCGAGGACTTCGACGCGATCGTCGTGTCC
CCGGGCCCCGGCAGCCCCGACCGGGAACGGGACTTCGGGATCAGCCGCCGGGCGATCACCGACAGCGGCCTGCCCGTCCTCG
GCGTCTGCCTCGGCCACCAGGGCATCGCCCAGCTCTTCGGCGGAACCGTCGGCC...
>rRED16-PLMVd
ATCGTTTAGGCACCCCAGGCTTTACACTTTATGCTTCCGGCTCGTATAATGTGTGGAATTGTGAGCGGATAACAATTTCAGA
ATTCGGGAAGAGTCTGTGCTAAGCACACTGACGAGTCTCTGAGATGAGACGAAACTCTTCCCTGTACAGATTCACACACAGG
AAACAGCTATGCGCACGCTTCTGATCGACAACTACGACTCGTTCACCCACAACCTGTTCCAGTACATCGGCGAGGCCACCGG
GCAGCCCCCCGTCGTCGTGCCCAACGACGCCGACTGGTCGCGGCTGCCCCTCGAGGACTTCGACGCGATCGTCGTGTCCCCG
GGCCCCGGCAGCCCCGACCGGGAACGGGACTTCGGGATCAGCCGCCGGGCGATCACCGACAGCGGCCTGCCCGTCCTCGGCG
TCTGCCTCGGCCACCAGGGCATCGCCCAGCTCTTCGGCGGAACCGTCGGCC...
>rRED17-ASBV-1
ATCGTTTAGGCACCCCAGGCTTTACACTTTATGCTTCCGGCTCGTATAATGTGTGGAATTGTGAGCGGATAACAATTTCAGA
ATTCGGGACGGGCCATCATCTATCCCTGAAGAGACGAAGGCTTCGGCCAAGTCGAAACGGAAACGTCGGATAGTCGCCCGTC
CCTGTACAGATTCACACACAGGAAACAGCTATGCGCACGCTTCTGATCGACAACTACGACTCGTTCACCCACAACCTGTTCC
AGTACATCGGCGAGGCCACCGGGCAGCCCCCCGTCGTCGTGCCCAACGACGCCGACTGGTCGCGGCTGCCCCTCGAGGACTT
CGACGCGATCGTCGTGTCCCCGGGCCCCGGCAGCCCCGACCGGGAACGGGACTTCGGGATCAGCCGCCGGGCGATCACCGAC
AGCGGCCTGCCCGTCCTCGGCGTCTGCCTCGGCCACCAGGGCATCGCCCAGCTCTTCGGCGGAACCGTCGGCC...

References and Notes

1. C. Adami, What is complexity? *Bioessays* **24**, 1085 (2002). doi:10.1002/bies.10192 Medline

2. J. D. Keasling, Manufacturing molecules through metabolic engineering. *Science* **330**, 1355 (2010). doi:10.1126/science.1193990 Medline

3. R. M. Hazen, P. L. Griffin, J. M. Carothers, J. W. Szostak, Functional information and the emergence of biocomplexity. *Proc. Natl. Acad. Sci. U.S.A.* **104**, (Suppl 1), 8574 (2007). doi:10.1073/pnas.0701744104 Medline

4. A. S. Khalil, J. J. Collins, Synthetic biology: Applications come of age. *Nat. Rev. Genet.* **11**, 367 (2010). doi:10.1038/nrg2775 Medline

5. J. M. Carothers, J. A. Goler, J. D. Keasling, Chemical synthesis using synthetic biology. *Curr. Opin. Biotechnol.* **20**, 498 (2009). doi:10.1016/j.copbio.2009.08.001 Medline

6. J. Zhang, M. W. L. Lau, A. R. Ferré-D'Amaré, Ribozymes and riboswitches: Modulation of RNA function by small molecules. *Biochemistry* **49**, 9123 (2010). doi:10.1021/bi1012645 Medline

7. H. Saito, T. Inoue, Synthetic biology with RNA motifs. *Int. J. Biochem. Cell Biol.* **41**, 398 (2009). doi:10.1016/j.biocel.2008.08.017 Medline

8. C. C. Liu, A. P. Arkin, Cell biology. The case for RNA. *Science* **330**, 1185 (2010). doi:10.1126/science.1199495 Medline

9. X. Chen, A. D. Ellington, Design principles for ligand-sensing, conformation-switching ribozymes. *PLOS Comput. Biol.* **5**, e1000620 (2009). doi:10.1371/journal.pcbi.1000620 Medline

10. W. J. Holtz, J. D. Keasling, Engineering static and dynamic control of synthetic pathways. *Cell* **140**, 19 (2010). doi:10.1016/j.cell.2009.12.029 Medline

11. Y. Benenson, RNA-based computation in live cells. *Curr. Opin. Biotechnol.* **20**, 471 (2009). doi:10.1016/j.copbio.2009.08.002 Medline

12. A. D. Garst, R. T. Batey, A switch in time: detailing the life of a riboswitch. *Biochim. Biophys. Acta* **1789**, 584 (2009). Medline

13. A. Deana, H. Celesnik, J. G. Belasco, The bacterial enzyme RppH triggers messenger RNA degradation by 5′ pyrophosphate removal. *Nature* **451**, 355 (2008). doi:10.1038/nature06475 Medline

14. J. R. Kelly *et al*., Measuring the activity of BioBrick promoters using an in vivo reference standard. *J. Biol. Eng.* **3**, 4 (2009). doi:10.1186/1754-1611-3-4 Medline

15. A. Saltelli *et al*., *Global Sensitivity Analysis: The Primer* (Wiley, Chichester, UK, 2008).

16. M. N. Win, C. D. Smolke, A modular and extensible RNA-based gene-regulatory platform for engineering cellular function. *Proc. Natl. Acad. Sci. U.S.A.* **104**, 14283 (2007). doi:10.1073/pnas.0703961104 Medline

17. M. Martick, W. G. Scott, Tertiary contacts distant from the active site prime a ribozyme for catalysis. *Cell* **126**, 309 (2006). doi:10.1016/j.cell.2006.06.036 Medline

18. K. H. Link *et al*., Engineering high-speed allosteric hammerhead ribozymes. *Biol. Chem.* **388**, 779 (2007). doi:10.1515/BC.2007.105 Medline

19. J. M. Carothers, J. A. Goler, Y. Kapoor, L. Lara, J. D. Keasling, Selecting RNA aptamers for synthetic biology: Investigating magnesium dependence and predicting binding affinity. *Nucleic Acids Res.* **38**, 2736 (2010). doi:10.1093/nar/gkq082 Medline

20. T. Pan, T. Sosnick, RNA folding during transcription. *Annu. Rev. Biophys. Biomol. Struct.* **35**, 161 (2006). doi:10.1146/annurev.biophys.35.040405.102053 Medline

21. H. M. Salis, E. A. Mirsky, C. A. Voigt, Automated design of synthetic ribosome binding sites to control protein expression. *Nat. Biotechnol.* **27**, 946 (2009). doi:10.1038/nbt.1568 Medline

22. H. Isambert, The jerky and knotty dynamics of RNA. *Methods* **49**, 189 (2009). doi:10.1016/j.ymeth.2009.06.005 Medline

23. Materials and methods are available as supporting material on *Science* Online.

24. J. L. Duffy *et al*., 4-aminophenylalanine and 4-aminocyclohexylalanine derivatives as potent, selective, and orally bioavailable inhibitors of dipeptidyl peptidase IV. *Bioorg. Med. Chem. Lett.* **17**, 2879 (2007). doi:10.1016/j.bmcl.2007.02.066 Medline

25. F. S. Sariaslani, Development of a combined biological and chemical process for production of industrial aromatics from renewable resources. *Annu. Rev. Microbiol.* **61**, 51 (2007). doi:10.1146/annurev.micro.61.080706.093248 Medline

26. B. F. Pfleger, D. J. Pitera, C. D. Smolke, J. D. Keasling, Combinatorial engineering of intergenic regions in operons tunes expression of multiple genes. *Nat. Biotechnol.* **24**, 1027 (2006). doi:10.1038/nbt1226 Medline

27. R. A. Mehl *et al*., Generation of a bacterium with a 21 amino acid genetic code. *J. Am. Chem. Soc.* **125**, 935 (2003). doi:10.1021/ja0284153 Medline

28. C. Flamm, I. L. Hofacker, Beyond energy minimization: Approaches to the kinetic folding of RNA. *Monatsh. Chem.* **139**, 447 (2008). doi:10.1007/s00706-008-0895-3

29. C.-H. T. Webb, N. J. Riccitelli, D. J. Ruminski, A. Lupták, Widespread occurrence of self-cleaving ribozymes. *Science* **326**, 953 (2009). doi:10.1126/science.1178084 Medline

30. H. H. Wang *et al*., Programming cells by multiplex genome engineering and accelerated evolution. *Nature* **460**, 894 (2009). doi:10.1038/nature08187 Medline

31. S. Ramsey, D. Orrell, H. Bolouri, Dizzy: Stochastic simulation of large-scale genetic regulatory networks. *J. Bioinform. Comput. Biol.* **3**, 415 (2005). doi:10.1142/S0219720005001132 Medline

32. J. Helton, J. Johnson, C. Sallaberry, C. Storlie, Survey of sampling-based methods for uncertainty and sensitivity analysis. *Reliab. Eng. Syst. Saf.* **91**, 1175 (2006). doi:10.1016/j.ress.2005.11.017

33. K. Salehi-Ashtiani, J. W. Szostak, In vitro evolution suggests multiple origins for the hammerhead ribozyme. *Nature* **414**, 82 (2001). doi:10.1038/35102081 Medline

34. C. D. Smolke, J. D. Keasling, Effect of gene location, mRNA secondary structures, and RNase sites on expression of two genes in an engineered operon. *Biotechnol. Bioeng.* **80**, 762 (2002). doi:10.1002/bit.10434 Medline

35. S. K. Lee, J. D. Keasling, A propionate-inducible expression system for enteric bacteria. *Appl. Environ. Microbiol.* **71**, 6856 (2005). doi:10.1128/AEM.71.11.6856-6862.2005 Medline

36. T. Lütke-Eversloh, G. Stephanopoulos, L-tyrosine production by deregulated strains of *Escherichia coli*. *Appl. Microbiol. Biotechnol.* **75**, 103 (2007). doi:10.1007/s00253-006-0792-9 Medline

37. A. M. Kierzek, J. Zaim, P. Zielenkiewicz, The effect of transcription and translation initiation frequencies on the stochastic fluctuations in prokaryotic gene expression. *J. Biol. Chem.* **276**, 8165 (2001). doi:10.1074/jbc.M006264200 Medline

38. H. Bremer, P. P. Dennis, Modulation of chemical composition and other parameters of the cell by growth rate. in Escherichia coli *and* Salmonella typhimurium*: Cellular and Molecular Biology* (American Society for Microbiology, Washington, DC, 1987), pp. 1527–1542.

39. I. Iost, J. Guillerez, M. Dreyfus, Bacteriophage T7 RNA polymerase travels far ahead of ribosomes in vivo. *J. Bacteriol.* **174**, 619 (1992). Medline

40. S. Arnold, M. Siemann Herzberg, J. Schmid, M. Reuss, Model-based inference of gene expression dynamics from sequence information. *Biotechnol. Fut.* **2005**, 89179 (2005).

41. J. Tomšic *et al*., Late events of translation initiation in bacteria: a kinetic analysis. *EMBO J.* **19**, 2127 (2000). doi:10.1093/emboj/19.9.2127 Medline

42. M. H. de Smit, J. van Duin, Translational standby sites: how ribosomes may deal with the rapid folding kinetics of mRNA. *J. Mol. Biol.* **331**, 737 (2003). doi:10.1016/S0022-2836(03)00809-X Medline

43. J. C. Penedo, T. J. Wilson, S. D. Jayasena, A. Khvorova, D. M. Lilley, Folding of the natural hammerhead ribozyme is enhanced by interaction of auxiliary elements. *RNA* **10**, 880 (2004). doi:10.1261/rna.5268404 Medline

44. A. Khvorova, A. Lescoute, E. Westhof, S. D. Jayasena, Sequence elements outside the hammerhead ribozyme catalytic core enable intracellular activity. *Nat. Struct. Mol. Biol.* **10**, 708 (2003). doi:10.1038/nsb959 Medline

45. D. W. Selinger, R. M. Saxena, K. J. Cheung, G. M. Church, C. Rosenow, Global RNA half-life analysis in *Escherichia coli* reveals positional patterns of transcript degradation. *Genome Res.* **13**, 216 (2003). doi:10.1101/gr.912603 Medline

46. H. Celesnik, A. Deana, J. G. Belasco, Initiation of RNA decay in *Escherichia coli* by 5′ pyrophosphate removal. *Mol. Cell* **27**, 79 (2007). doi:10.1016/j.molcel.2007.05.038 Medline

47. H. El-Samad, H. Kurata, J. C. Doyle, C. A. Gross, M. Khammash, Surviving heat shock: control strategies for robustness and performance. *Proc. Natl. Acad. Sci. U.S.A.* **102**, 2736 (2005). doi:10.1073/pnas.0403510102 Medline

48. S. E. McDowell, D. Rueda, N. Walter, How loop loop interactions in a transacting hammerhead ribozyme enhance function. *RNA Soc. Ann. Meeting* **11**, 379 (2006).

49. D. M. Long, O. C. Uhlenbeck, Kinetic characterization of intramolecular and intermolecular hammerhead RNAs with stem II deletions. *Proc. Natl. Acad. Sci. U.S.A.* **91**, 6977 (1994). doi:10.1073/pnas.91.15.6977 Medline

50. C. de Silva, N. G. Walter, Leakage and slow allostery limit performance of single drug-sensing aptazyme molecules based on the hammerhead ribozyme. *RNA* **15**, 76 (2009). doi:10.1261/rna.1346609 Medline

51. I. L. Hofacker, Vienna RNA secondary structure server. *Nucleic Acids Res.* **31**, 3429 (2003). doi:10.1093/nar/gkg599 Medline